Egypt. J. Chem. **Vol. 66**, No. 5 pp. 129 - 150 (2023)

Egyptian Journal of Chemistry

http://ejchem.journals.ekb.eg/

Implication of Lower Cretaceous Kaolinitic Clay Deposits Characterization in Industry, Case: West Central Sinai, Egypt

Ahmed Abdelhalim[1,*], Ahmed Melegy[2], Dina Othman,[3]

[1] *Department of Geology, Faculty of Science, Cairo University, Giza, Egypt*
[2] *Department of Geological Sciences, National Research Center,Giza,Egypt*
[3] *Ahmed Othman Co. for Mining, Maadi, Egypt*

Abstract

This study examines the physical, geochemical, and mineralogical characteristics of a few kaolin resources in West Central Sinai that are found within substantial Malha Formation (Lower Cretaceous) sandstone layers. Kaolin samples were characterised using microscopic, SEM, XRD, and ICP-MS techniques. All of the tested samples from the researched kaolin resources include kaolinite as their predominant clay mineral. Illite and smectite are occasionally found as minor clay elements, while dickite and/or halloysite are subordinate TO clay minerals. The following non-clay minerals have been identified: quartz, gypsum and hematite. Ferrugination occurs mostly at the upper boundaries of the kaolin lenses in contact with the overlying sandstone beds suggesting a possible supergene activity. The high Al2O3/SiO2 ratio of 0.53 indicates the high quality of Cretaceous kaolin deposits in Sinai. The kaolin of the lower lens in Rueikna and upper lens in Salia contains Si/Al molecular ratio of 0.9 which suggests a high grade of kaolin in these two lenses. A greater input of LREE is a characteristic of the Cretaceous kaolin (Monazite signature). Although all of the investigated kaolin deposits have very high CIA indices (97.4 and 99.2), implying significant limits of chemical weathering, none of them exhibit anomalous Ce.The Lower Cretaceous kaolin of Sinai does not meet the requirements of the refractory and paper industries, but beneficiation might be able to solve this problem. However, some lenses have high-grade kaolin and are nominated for the regional refractory industry because they have low levels of radioactivity, iron oxides, magnesium oxides, sodium oxides, calcium oxides, and potassium oxides. All of the kaolin lenses from the studied areas can be used in local ceramic manufacturing, and the high-grade kaolin of Sinai satisfies the criteria necessary for ceramic manufacture in the global market.

Keywords: Kaolin deposits; Rueikna; Salia; Shushet Abu El-Nimran; Sinai Peninsula

1. Introduction

The world's most significant and practical industrial minerals include kaolin deposits. Our society uses clays and clay minerals widely in a variety of contexts. They are crucial for many industrial and environmental applications as well as geology, agriculture, building, and engineering. Traditional uses include the decolorization, construction industry, ceramics, paper, paint, plastics, drilling fluids, foundry bondants, chemical carriers, liquid barriers, and catalysis. (Zegeye *et al.*, 2013; Hafez *et al*., 2017; Chargui *et al*., 2018; Valaskova *et al*., 2018; Mebrek *et al*., 2019; Ababneh *et al*., 2020; Mamudu *et al*., 2020; Refaie *et al*., 2020). Kaolin can also be used to increase yield of rice when it is added to the soil (Samidurai *et al*., 2002). It is also have been recently used for conserving soil water and removing of pollutants (Glenn, 2016; AbdAallah, 2019; Mustapha *et al*., 2019).

One of the most commonly used industrial minerals, kaolin is a strategic raw material in numerous sectors, with a global production of about 25 million tonnes (Wilson, 2003). Kaolin is widely utilised in the ceramics, rubber, paint, plastics, and pharmaceutical industries, despite being primarily employed in the production of paper, which accounts for around 75% of global production (Murray, 2000; Spinola et al., 2019). Kaolin is a common ingredient in many different cosmetic products, including foundations, makeup bases, mascaras, face powders, blushers, and eye shadows. Kaolin was reportedly utilised in 509 distinct cosmetic products in the USA in 1998. (CIREP, 2003).

Kaolin has a wide range of industrial applications, however each technological use requires a different set

*Corresponding author e-mail: ahmedabdelhalim@cu.edu.eg; (Ahmed Abdelhalim).
Receive Date: 04 August 2022, Accept Date: 20 August 2022.
DOI: 10.21608/EJCHEM.2022.153794.6670
©2019 National Information and Documentation Center (NIDOC).

of qualities. The geological conditions that lead to the formation of the deposits, as well as their bulk mineralogical, chemical composition, and crystal order (Cases, et al., 1982 and 1986; Martin, 1994; Pinheiro, et al., 2005; El-Kammar, et al., 2017; Maia et al., 2019), as well as their physical characteristics like colour and firing characteristics, determine these properties (Bloodworth, et al.,1993; Gamiz, et al., 2005; Siddiqui, et al., 2005; Hadi and Hussein, 2019; Marfo et al., 2020). Kaolin has several qualities that are useful in medicine. It is a superior adsorbent that can capture not only lipids and proteins but also viruses and bacteria (Wallace et al., 1975), and it is employed in medical therapy as a local and gastrointestinal adsorbent (Lipson and Stotzky, 1983). However, Egypt has significant economic kaolin reserves in many areas, including the Sinai, the Red Sea coast, and Kalabsha near Aswan. The current study focuses on the makeup and origin of the Cretaceous kaolin resources found in the Sinai regions of Shushet Abu El-Nimran, Rueikna, and Salia. However, Egypt has significant economic kaolin reserves in numerous areas, including the Sinai, the Red Sea coast, and Kalabsha near Aswan. The current study focuses on the makeup and origin of the Cretaceous kaolin resources found in the Sinai regions of Shushet Abu El-Nimran, Rueikna, and Salia.

Kaolin deposits of Abu-Zenima area (West Central Sinai), El Tih Plateau at Gebel Shushet-Abu El Nimran, Gebel Rueikna and Gebel Salia, are mainly interbedded within sandstones of Cretaceous age (Abdallah, *et al*., 1963; Abu-Zeid, 2008). The kaolin deposits in Sinai have been the subject of numerous investigations. These research covered a variety of topics, including their mineralogical and chemical composition, physical and ceramic qualities, and their mineralogy (Morsy and Shata 1992; Boulis and Attia 1994, Yanni 1988; Hegab et al. 1992; Rashed and Amer 1994; Awad 1995; Ramadan et al., 2013). A complicated geological history with one or more superimposed alteration events is common in sedimentary kaolin deposits (e.g., Pruett and Pickering 2006; Baioumy and Gilg 2011). However, the weathering processes in lithologically distinct source locations as well as the mineral sorting during transport and deposition are largely reflected in their mineralogical and geochemical features (e.g., Pruett and Murray 1993).

Therefore, the present work focuses on the geochemical and mineralogical composition of Early Cretaceous kaolin deposits of Shushet Abu El Nimran, Rueikna and Salia in Sinai (Fig. 1). In addition to its implication in industrial purposes.

Fig. (1): Location map of the studied areas of the kaolinitic clay of Sinai, Gebel Shushet-Abu El Nimran, Gebel Rueikna and Gebel Salia, Sinai.

2. Geologic setup

The Malha, Galala, Halal, and Wata formations are part of the Lower Cretaceous sedimentary sequences in west-central Sinai, according to the current field investigation and reconnaissance survey (Fig. 4). The Cretaceous kaolinitic clay deposits in Sinai are found in the base Malha Formation, which is primarily made up of grey, ferruginous cross-bedded sandstones with a few interbeds of green silty shales and calcareous sandstones (Abdallah et al., 1963, Abu- Zeid, 2008; Wanas, 2011).

The Lower Cretaceous sedimentary kaolinitic clays of Shushet Abu El-Nimran, Rueikna and Salia belong to the Malha Formation in N and NE of Abu Zenima. These resources cover an area between latitudes; 29º 10' 51" and 29º 12' 01" N and longitudes; 33º 18' 02" and 33º 26' E (Fig. 2). The studied area in Shushet Abu El-Nimran kaolinitic clay deposits occur between latitudes; 29º 10' 51" and 29º 12' 01" N and longitudes; 33º 18' 02" and 33º 18' 58" E. While in Rueikna and Salia they occur between latitudes; 29º 10' 51" and 29º 12' 01" N and longitudes; 33º 25' 01" and 33º 26' E. While Malha Formation is composed of four kaolinitic clay beds assigned as A, B, C and D from base to top. Only the upper two kaolinitic clay beds have been encountered in the studied areas (Fig. 3).

The studied kaolinitic deposits of the West Central Sinai are located within the Lower Cretaceous Malha Formation (Fig. 3). Field observations indicate that the studied Lower Cretaceous kaolin deposits contain high percentage and large grain size of detrital quartz fragments.

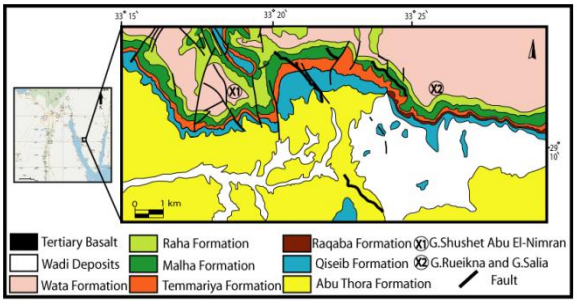

Fig. (2): *Location and geological map of kaolinitic clay study areas at Shushet Abu El-Nimran, Rueikna and Salia, modified after Geological Survey of Egypt, 1994.*

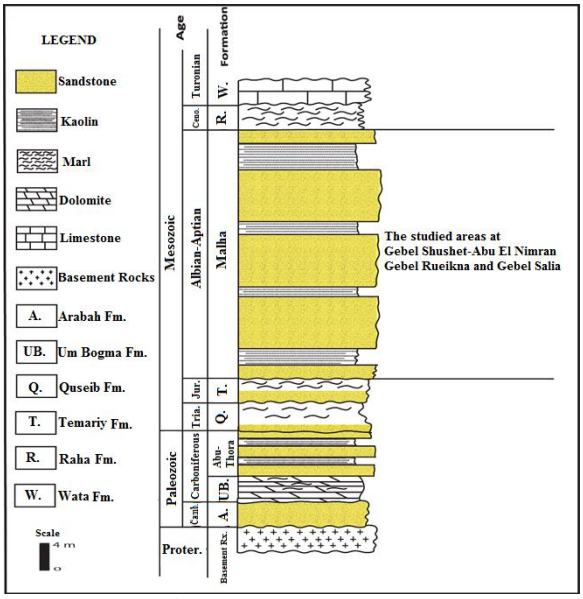

Fig. (3): *Litholog of West Central Sinai showing the kaolinitic clay bearing formation (Malha Formation) in the studied areas, El Tih-Plateau, West- Central Sina, after Geological Survey of Egypt, 1994.*

Kaolinite beds of different thickness are separated from each other by relatively thick sandstone beds up to 8 m in thickness. The kaolin and sandstone (yellow to reddish in color) are found to be barren of any mega-fossils, as of Shushet Abu El-Nimran area. Also the base of the stratigraphic section in Rueikna and Salia areas, a relatively thick Malha (sandstone) Formation is located. It is made up of non-fossiliferous, friable, pinkish white sandstones. Rueikna and Salia kaolinitic clay deposits are interbedded within the sandstone of the Malha Formation and occur in the form of two flat, separated lenses, named from base to top; C and D lenses. The thickness of these kaolin lenses ranges from 10 to 11 m. (Figs. 4-6).

The following is brief discussion on the stratigraphy of the sedimentary succession in Shushet Abu El-Nimran (Fig. 4), Rueikna (Fig. 5) and Salia (Fig. 6) areas. The lateral and vertical variation in facies has been considered during sampling and field observations. Based on these field observations, a compiled lithostratigraphic section of these studied areas has been constructed to show the precise location of the collected samples.

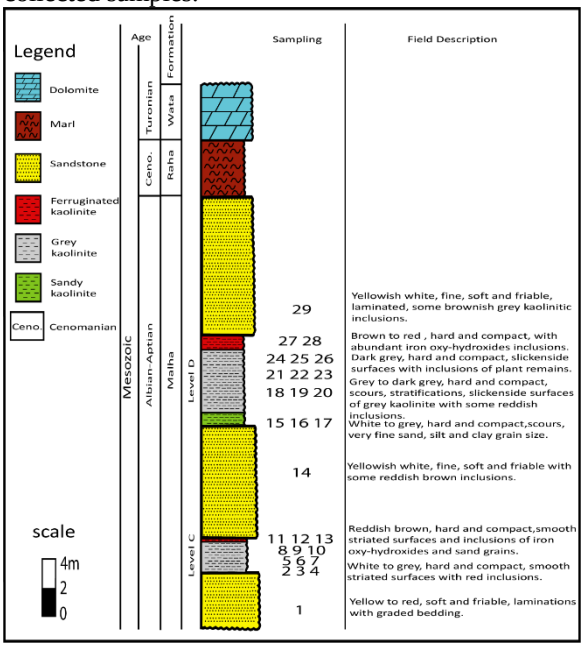

Fig. (4): Litholog of Shushet Abu El-Nimran area in El Tih- Plateau, West Central Sinai showing the position of kaolinitic clay bearing Malha Formation

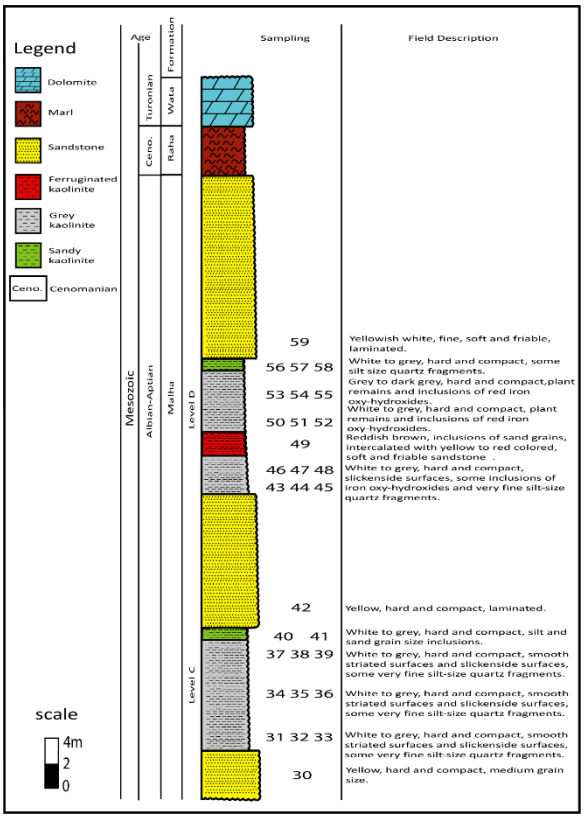

Fig. (5): Litholog of Rueikna area in El Tih- Plateau, West Central Sinai showing the position of kaolinitic clay bearing Malha Formation

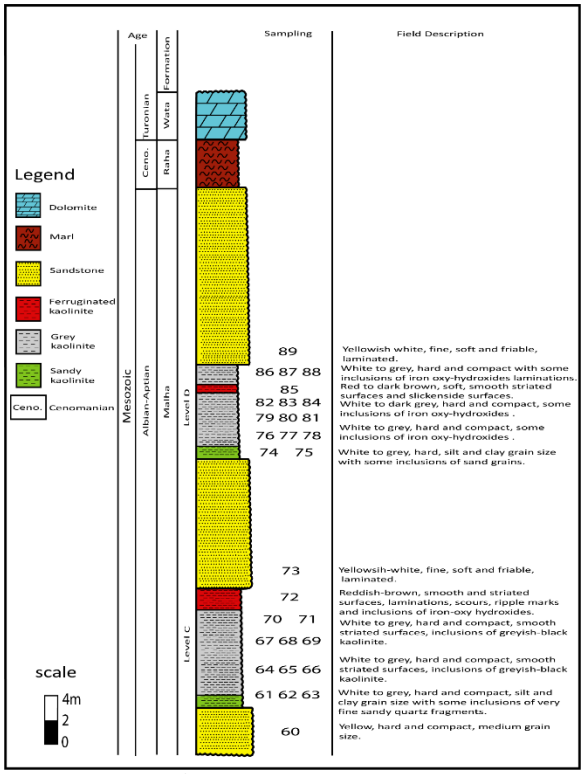

Fig. (6): *Litholog of Salia area in El Tih- Plateau, West Central Sinai showing the position of kaolinitic clay bearing Malha Formation*

2.1 Shushet Abu El-Nimran kaolin deposits:

The lower kaolinitic clay lens (level C) has a thickness of 2.5 m and can only be exploited by open mines, where it has a surface exposure of kaolinitic clay deposit (Fig. 7). Also, the kaolin lens of level C grades from white to grey fresh kaolinitic clay at the bottom to thin layer of reddish brown kaolinitic clay (ferruginous kaolinitic clay). The upper kaolinitic clay lens (level D) has a thickness of 6.5 m and can only be exploited by open mines as it has a surface exposure of kaolinitic clay deposit (Fig. 9). The kaolinitic clay deposit of level D lens grades from white to grey sandy kaolinitic clay at the bottom to grey to dark grey of the fresh kaolinitic clay in the middle part while the upper part occurred as completely red ferruginous kaolin. Smooth striated polished surface (Fig. 8) is characteristic feature of the whitish grey kaolinitic clay and some ferruginous kaolinitic clay of the middle part which indicates that there was little free silica during the time of deposition. So, the upper part of level D kaolinitic clay lens is considered by its lowest grade due to the presence of higher proportion of iron-oxides as inclusions and interlaminations alteration within the deposit (Fig. 10)

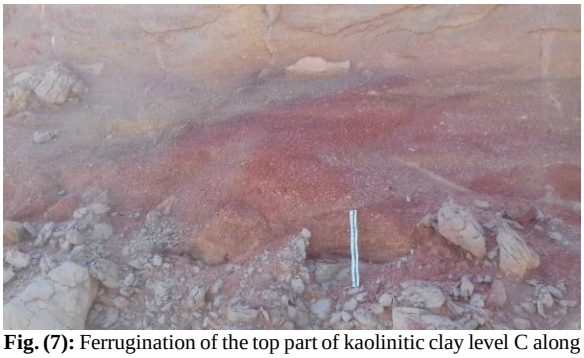

Fig. (7): Ferrugination of the top part of kaolinitic clay level C along the contact with the overlying Malha sandstone bed at Shushet Abu El-Nimran area.

Fig. (8): Red ferruginated Malha sandstone alternating with yellow sandstone overlying level C kaolinitic clay at Shushet Abu El-Nimran area.

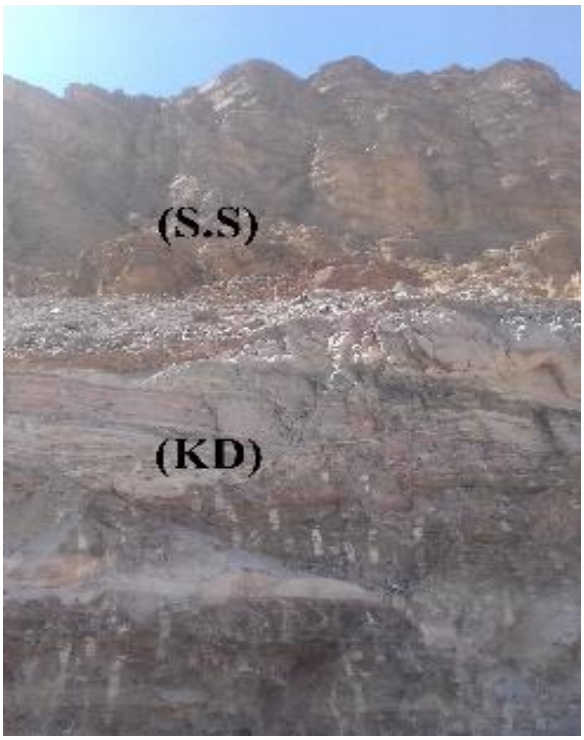

Fig. (9): Sandstone bed (S.S) overlying kaolinite lens (level D) (KD), at Shushet Abu El-Nimran area.

Fig. (10): Ferrugination of kaolinite in top part of level D lens along contact with the overlying sandstone bed, at Shushet Abu El-Nimran

2.2 Rueikna kaolin deposits:

Rueikna kaolinitic clay lenses show obvious vertical variation in color and intercalated sandstone beds which is similar to Shushet Abu El-Nimran area. Due to ferrugination of kaolinitic clay deposits, especially those in contact with the intercalated sandstone bed at the lower lens, show obvious repetition of vertical variation in the kaolinitic clay color.

The lower kaolinitic clay lens at Rueikna (Level C), is formed of kaolinitic clay of white, whitish-grey and dark grey color. The top part of this lens in contact with the overlying sandstone bed is sandy kaolinite (Fig. 11). Level C kaolinitic clay lens has a thickness of 10 m and can be exploited by an open cast operation as it is properly outcropping.

The upper kaolinitic clay lens at Rueikna named Level D, is larger in thickness, about 11 m. This kaolinitic clay varies in color. The lower part is composed of grey colored kaolinite, while the middle layer is composed of reddish ferruginated kaolinite in contact with intercalated sandstone bed and the top layer is formed of grey to dark grey kaolinite containing plant remains (Fig. 12), indicating the presence of high content of organic matter, followed by sandy kaolinite layer in contact with the overlying sandstone bed.

Ferrugination of Rueikna kaolinitic clay deposits is only shown in the upper lens. The kaolinitic clay in the ferruginated zones is variable in color, due to the variable intensity of alteration and pigmentation of iron-oxyhydroxides within the lens. The change in color results from alternating variable colored yellow and reddish bands with relics of original white and grey kaolinitic clay bands. This ferrugination is observed on kaolinitic clay in contact with the overlying intercalated varicolored sandstone bed.

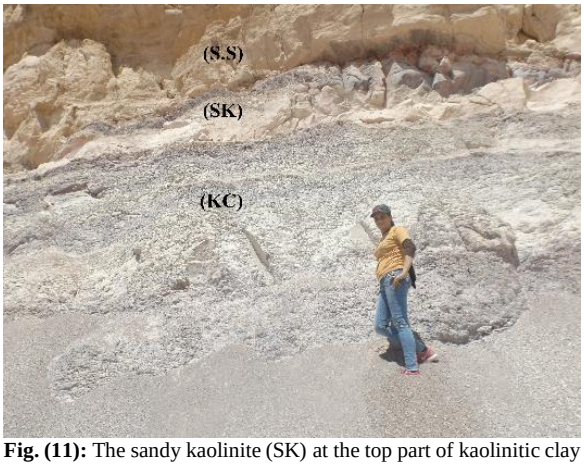

Fig. (11): The sandy kaolinite (SK) at the top part of kaolinitic clay lower lens (level C)(KC) in contact with the upper sandstone (S.S) bed at Rueikna area.

Fig. (12): Plant remains and ferrugination shown in kaolinitic clay sample collected from the top part of the upper lens (level D) bed at Rueikna area

2.3 Salia kaolin deposits:

Like kaolinitic clay lenses at Shushet Abu El-Nimran and Rueikna, kaolinitic clay lenses at Salia area show obvious vertical variation in color and in the intercalated sandstone beds. The observed repetition of the vertical variation in color of kaolinitic clay deposits from grey to red is due to ferrugination of these deposits. Due to the presence of many faulted blocks in Salia area, each kaolinitic clay lens has to be investigated separately around this area in order to obtain accurate estimation about the two kaolinitic clay beds in this area.

Ferrugination of Salia kaolinitic clay deposits is heterogeneous. The intensity of alteration and pigmentation with iron oxy-hydroxides is variable within the different lenses. The kaolinite in the ferruginated zones is variable in color. The change in color results from alternating variable colored yellow and reddish bands with relicts of original white and grey kaolinite bands. In level C kaolinitic clay lens, ferrugination occurs as alternating beds of red kaolinite and grey kaolinite and concentrate along fault planes and also as red kaolin intercalations

specially in the top part of level C kaolin lens (Fig. 13). However, the reddish/grey kaolinite bands, as well as iron oxy-hydroxides enclosures have been observed within the kaolinite occupying the top parts of the higher Level D kaolin lens (Fig. 14).

Fig. (13): Ferruginated kaolinite (level C) at Salia area.

Fig. (14): Ferruginated kaolinite at the middle part of level D kaolinitic clay lens, at Salia area

3. Samples and methods

To represent the various kaolin lenses and the sandstone that serves as their host in the study locations, 88 samples were gathered. The main petrographical and mineralogical features are studied by petrographic polarizing microscope. Scanning Electron Microscope (SEM), model quanta 250 Field Emission Gun (FEG) attached with Energy Dispersive X-ray (EDX) analyzer, at accelerating voltage 30 kV, was used. The instrument is housed in the Central Laboratories of the Egyptian Mineral Resources Authority (EMRA). The X-ray diffraction analysis was conducted on six whole-rock samples using Cu Kα radiation and Ni filter at scanning rate of 2° (2θ) per minute. The used instrument is housed in the Central Laboratories of the Egyptian Mineral Resources Authority (EMRA) of model; P.W. 1930, at voltage 40 kV and current 30 mA. Since the microscopic examination indicates that the studied kaolin contains about 80%, in average, of clay-size fraction, the X-ray analysis was done on whole-rock samples.

One kaolin sample from each mapped lens was chosen from the six bulk kaolin samples for XRD study, and four comparably high-grade kaolin samples were chosen for SEM investigation. Twenty samples from the investigated kaolin deposits have been chosen for chemical analysis. These examples depict the lateral and vertical differences of the kaolin lenses that have been encountered. The Lower Cretaceous kaolin deposits were represented by twenty samples; seven samples from Shushet Abu El-Nimran, seven samples from Rueikna, and six samples from Salia areas (Tables 1, 2 and 3). The ratio of alumina/silica and ratios between the common isovalents, such as Zr/Hf, Nb/Ta, Y/Ho and Th/U, are listed in table (4), which involves also the LREE/HREE ratio and ΣREE. The tetrad effect (t1, t3 and t4) of the REE was calculated but it is always of insignificant value.

The chemical analysis of the major, trace and rare earth elements (REE) was conducted on whole rock samples using the inductively coupled plasma-mass spectrometric analysis (ICP-MS) in the Acme lab of Vancouver in Canada (Tables 1, 2 and 3). The obtained data are used to interpret the genetic and diagenetic bearings of the studied kaolin resources.

3.1. Discussion

The main objective of the SEM examination is to characterize the main microstructures and the diagenetic modifications in four kaolin samples representing some kaolin lenses of the L. Cretaceous resources. The SEM Petrology Atlas of Welton (1984), with provision of the EDX data, supported the mineral identification. Six bulk kaolin samples have been chosen for X-ray analysis.

The information gathered shows that kaolinite is the dominant clay mineral in all of the samples that were examined. Illite and smectite are occasionally found as minor clay elements, while dickite and/or halloysite are secondary TO clay minerals (Figs. 15-20). Some non-clay minerals have been identified as quartz, gypsum, and hematite.

The intensities and sharpness of kaolinite have been measured on the basal reflection of kaolinite in the obtained diffractograms. The obtained data indicate a moderate to well crystalline nature of kaolinite. In general, the intensity of quartz diffractions increases at the expense of kaolinite peaks. The microscopic examination confirms this observation, where detrital quartz increases at intervals of active terrestrial input to the depositional basin (Figs. 15-20).

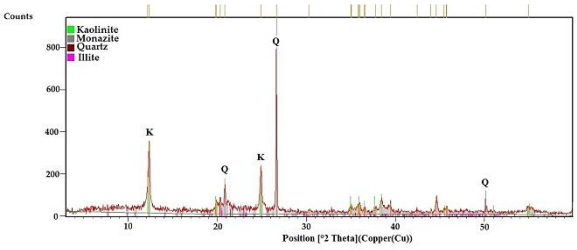

Fig. (15): XRD patterns of the grey kaolin (sample no. 2) collected from the lower lens of the Lower Cretaceous Shushet Abu El-Nimran kaolin deposit

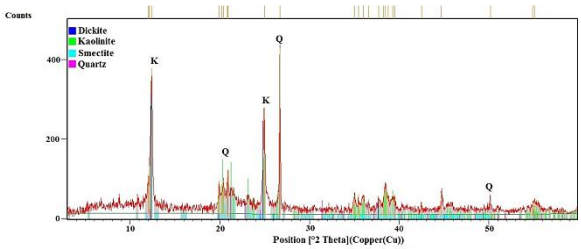

Fig. (16): XRD patterns of grey kaolin (sample no. 22) collected from the upper lens of the Lower Cretaceous Shushet Abu El-Nimran kaolin deposit

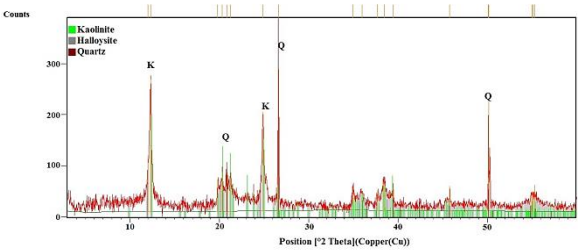

Fig. (17): XRD patterns of grey kaolin (sample no. 35) collected from lower lens of the Lower Cretaceous Rueikna kaolin deposit

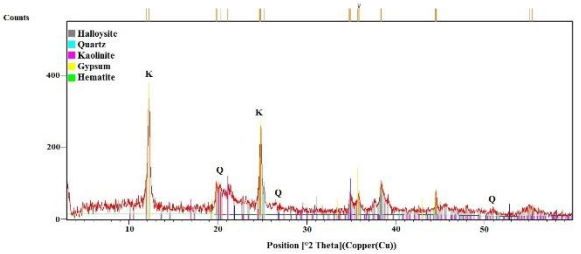

Fig. (18): XRD patterns of grey kaolin (sample no. 47) collected from the upper lens of the Lower Cretaceous Rueikna kaolin deposit

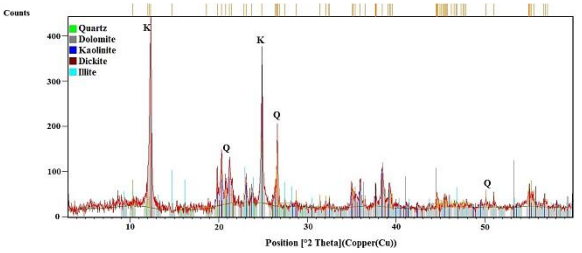

Fig. (19): XRD diffractogram of grey kaolin (sample no. 65) collected from the lower lens of the Lower Cretaceous kaolin of Salia kaolin deposit

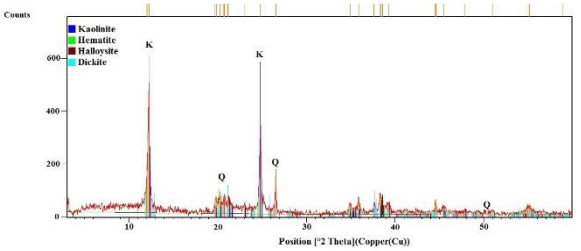

Fig. (20): XRD patterns of the grey kaolin (sample no. 77) collected from the upper lens of the Lower Cretaceous Salia kaolin deposit

About seven thin and thin-polished sections of kaolin samples collected from the lenses under investigation which are representing the different lithologies were examined. In general, the ferruginous kaolin variety occupies the topmost part of some lenses and middle parts of other lenses. Different amounts of organic content, major clay-size fractions (> 75%, by volume), detrital quartz grains (5 to 25%), and levels of ferrugination are present in the investigated kaolin. These features affect the color and compactness of the studied kaolin deposits. Since color and clay quotient are pinpointing technical parameters, that control kaolin quality and price, they will be respected in the forthcoming discussions. The following is short discussion on the main petrographical and mineralogical features of the studied kaolin resources.

3.1.1 *Shushet Abu El-Nimran Kaolin Deposits*

The XRD analysis indicates that kaolinite is quantitatively the main clay mineral constituent of the Shushet Abu El-Nimran deposits. However, dickite, illite and smectite have also been recorded as inconsequential clay constituents (Figs. 15 and 16). The detected non-clay minerals include quartz in variable concentrations and minor amount of the accessory mineral monazite.

However, the high grade kaolin of upper lens of Shushet Abu El-Nimran (sample no. 22) produces weak reflections related to dickite and smectite in addition to the major kaolinite (*see* Fig. 16). Similar variations in clay mineralogy have also been recorded in the lower kaolin lens (Fig. 15). The intensity of quartz peaks varies considerably from one sample to another and is more intense in the lower lens than in the upper one. However, based on the obtained XRD and the detailed microscopic examination, it is possible to mention that the kaolin deposits of Shushet Abu El-Nimran are enriched in quartz (3-20%) relative to those of the Salia deposits (3-10%).

In Shushet Abu El-Nimran, ferrugination is particularly noticeable on the topmost kaolin lenses, which raises the possibility of a diagenetic supergene episode. Although goethite and limonite are also found, hematite staining is the main reason of this ferrugination. Both kaolin lenses exhibit significant upward coarsening; the topmost lens is best described as ferruginous sandy-silty kaolin, while the middle lens has a higher proportion of detrital quartz (silt to fine sand sizes).

Lower kaolin lens: This kaolin lens is mineable at present. Similar to the other lenses, it displays marked variation in facies as a result of changing energy of deposition. Its lowermost part is white to grey kaolin (24.3%, alumina), but changes upwardly to better grade of white kaolin (29.55-30.6%, alumina). The topmost part of the lens is of lower grade (28.01%, alumina) compared to the middle part.

Kaolin in the middle lower lens is pale colored quartz-poor commercial silty kaolin (Fig. 21).

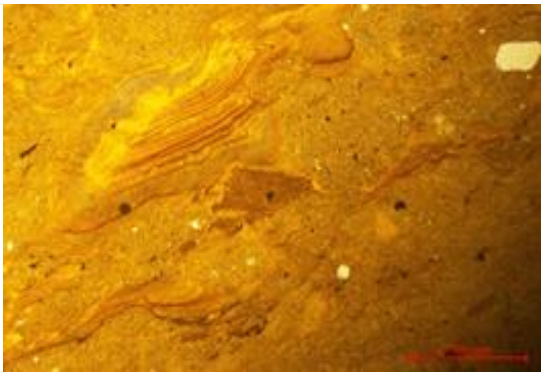

Fig. (21): High grade pale-colored kaolin showing abundant flaky appearance with preferred orientation. Few fine quartz grains are disseminated. PPL.

Upper kaolin lens: like the lower lens, this lens displays upward coarsening due to changing energies during deposition. The bottom of the lens is low grade (28.49%, alumina), multicolored silty kaolin containing coarse clastics of quartz, feldspars and plant remains (Fig. 22). The middle part of the lens is of a whitish grey color and a better grade with 31.32% alumina content. The uppermost part is the lowest in grade with alumina content of 27.40% and is also markedly enriched in clastics (up to 20%) of different sizes where diameter ranges from 0.03-0.15 mm (Fig. 23).

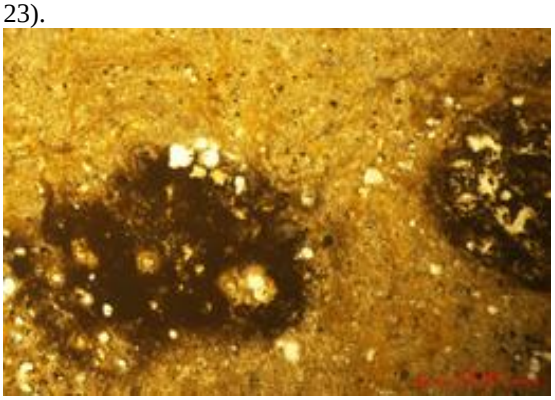

Fig. (22): Multicolored silty kaolin containing blackish enclaves enriched in organic carbon and relatively rich in detrital grains of different sizes. PPL.

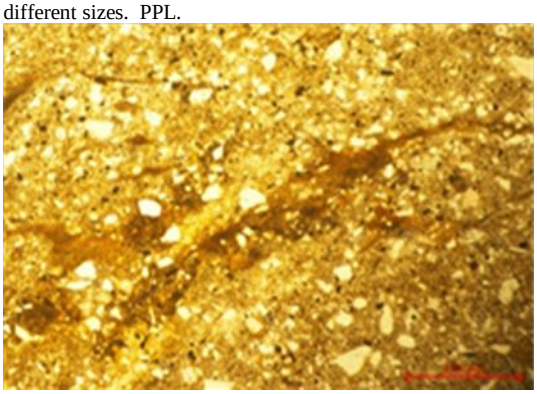

Fig. (23): Pale-colored fine sandy kaolin rich in detrital quartz and thin flakes of plant remains. PPL.

Scanning Electron images of Shushet Abu El-Nimran, upper lens (sample number 22) and the lower lens (sample number 5). At the upper lens (sample number 22), it is shown that the well crystalline six-sided book-like flakes of kaolinite represent more than 75% of the sample with well crystalline monocrystalline quartz grains. Few scattered monocrystalline quartz grains are preferentially accumulated along lamination in the lower lens. The large void spaces in the rock, explain the marked permeability of this kaolin (Fig. 24). While at the lower lens (sample no.5) are shows moderately to well crystalline book-like structure of kaolinite (Fig. 25).

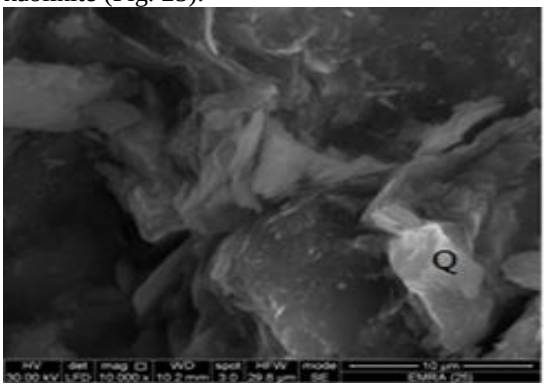

Fig. (24): BSE image of high grade kaolin of the upper lens of Shushet Abu El-Nimran, showing book-like structure of kaolinite, with very few small size quartz grains (Q). Note the large pore space in the lower left corner of the image.

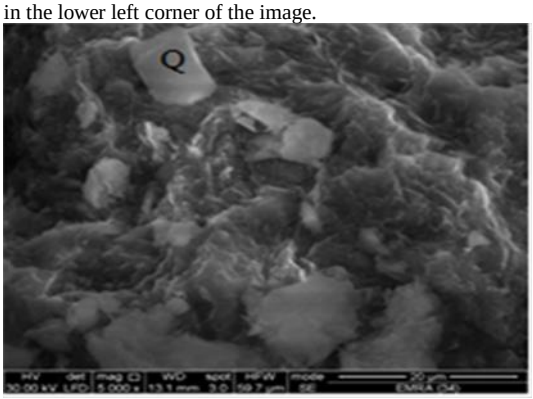

Fig. (25): BSE image of the high grade whit kaolin, of the lower lens of Shushet Abu El-Nimran, showing book-like structure of kaolinite forming lamination with few scattered monocrystalline quartz-grains (Q).

3.1.2 *Rueikna Kaolin Deposits*

In hand specimens, the kaolin of Rueikna is grey in color with brownish tints and some plant remains. Microscopically, the rock is composed of pale brown to brownish grey granules of kaolinite. It is highly enriched in black and reddish brown structurless plant remains. Organic matter may also exist as black opaque patches up to 1 mm in diameter, partially replaced by secondary chalcedonic-quartz showing grey first order interference colors and wavy extinction. Black colored streaks and lensoidal

materials parallel to lamination are also recorded (Fig. 26). Abundant detrital quartz (up to 20%) of silt to sand sizes is disseminated in the kaolinite matrix (Fig. 27). The X-ray analysis indicates that kaolinite is the main clay mineral with occasional halloysite, while quartz is the main non-clay mineral with minor presence of hematite and gypsum.

Fig. (26): Brownish-grey, organic-rich, sandy kaolin of the topmost part of the upper lens in Rueikna: Notice the preferred orientation of quartz clastis. PPL.

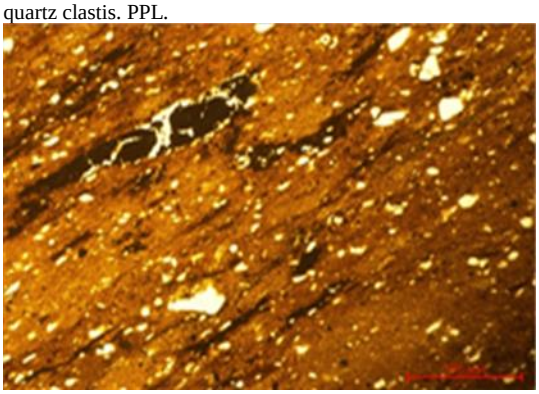

Fig. (27): Sandy kaolin of the same lens showing the preferred orientation of both plant remains and angular detrital quartz of different sizes. PPL.

3.1.3 *Salia Kaolin Deposits*

The XRD analysis and the petrographic examination indicate that the lower lens of Salia kaolin has distinctive muddy facies, where the clay-size fraction dominates with subordinate detrital fraction. The XRD analysis proposes that the lower lens contains occasional quartz and insignificant dickite and illite, in addition to weak reflections that can be interpreted to dolomite (Fig. 19). However, the kaolin of the upper lens is essentially composed of kaolinite, while kaolinite is quantitatively the main clay mineral constituent of the upper Salia kaolin deposits. However, dickite, and halloysite, have also been recorded as inconsequential clay constituents (Fig. 20). The detected non-clay minerals in Salia kaolin samples include quartz in variable concentrations, in addition to minor hematite.

Microscopically, the kaolin in the upper lens is silty. It is primarily composed of detrital quartz and clay-sized kaolinite particles. The analysed samples' detrital portion contains opaque grains and prismatic high relief zircon (Fig. 28). The top lens's kaolin deposits contain organic materials in varying amounts and forms (Fig. 29). During deposition, this organic material is documented in the various stratigraphic strata.

Fig. (28): Grey upper Salia kaolin lens. The organic matter together with leaching streaks oriented along lamination. Plane Polarized Light (PPL).

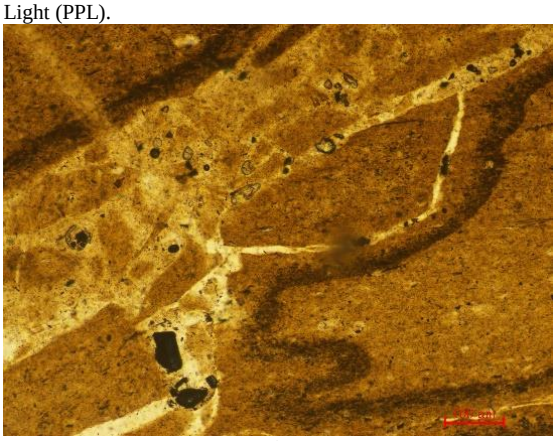

Fig. (29): Irregular network of siliceous veinlets cut across grey kaolin of the lower kaolin lens in Salia area. Opaque heavy minerals, zircon (high relief) and quartz grains associate the veinlets. Plane Polarized Light (PPL).

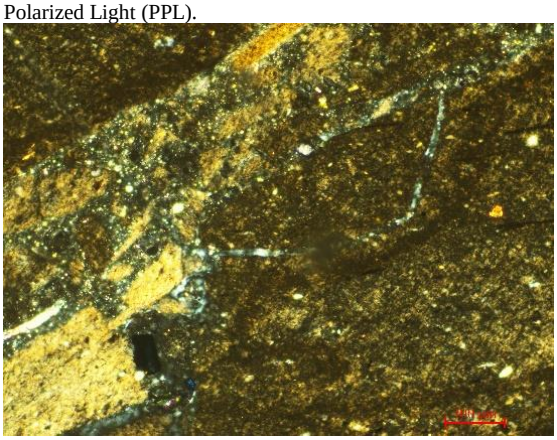

Fig. (29*): Irregular network of siliceous veinlets cut across grey kaolin of the lower kaolin lens in Salia area. Opaque heavy minerals, zircon (high relief) and quartz grains associate the veinlets. Crossed Nicols (CN).

The megascopic examination suggests that the rock at the bottom of the lens are grey and plastic in nature. Going upward, the middle layer in the lens, the kaolin becomes lighter in color. The red ferruginous kaolin occupies the topmost layer of the lower lens and the middle part of the upper one. However, the organic matter concentrates along lamination, but the long axis of the large fragments is often parallel to the bedding plane. Very finely laminated black to dark brown streaks, thin shreds and irregular lenses "probably of organic origin" are strung out parallel to the bedding planes and also cutting across forming discontinuous lenses (Fig. 28) and clouds mask the kaolinite particles. Sometimes, the grey coloration by organic matter is mixed with reddish brown shades resulting from staining by ferruginous materials. The removal of organic matter by heating at 420°C enhance the remaining color related to ferrugination. The kaolin deposits are frequently dissected by brighter colored veinlets and streaks of chalcedonic-quartz displaying wavy extinction of 1st order interference colors (Fig. 29 &29*****). The SEM examination of such masses proposes their organic composition (Fig. 30). The obtained EDX data suggest organic composition of such masses, where C appears as major component with the kaolinite ingredients as represented by Al, Si and Ti. Iron is not detected in the analysis (Fig. 31).

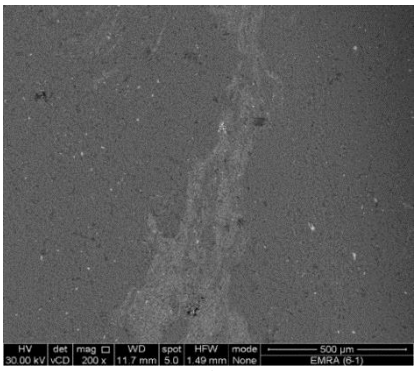

Fig. (30): BSE image of dark brown lensoidal substance appearing in Fig. 48, of brownish light grey organic mass embedded within kaolin matrix. Lower Cretaceous kaolin of the upper lens in Salia.

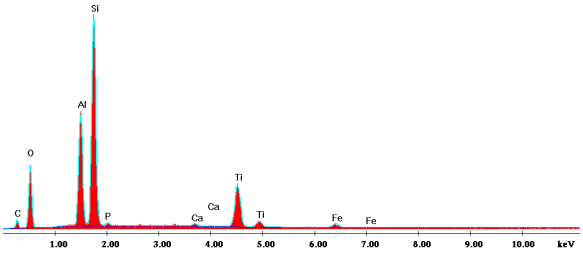

Fig. (31): EDX spectrum of the organic-rich mass.

Measuring the sharpness of kaolinite, based on the width of its basal reflection at its mid-height, indicates a moderate to a well crystalline nature. The presences of well-defined sharp and clearly resolved peaks of kaolinite support the deduced moderate-well crystallinity of the examined Salia kaolinite. The SEM examination confirms the well define edges and outlines of hexagonal shape of the kaolinite composing the lower lens of Salia kaolin (Fig. 32), compared to finer intergranular pseudo-hexagonal kaolinite crystals in the light grey kaolin of the upper lens (Fig. 33).

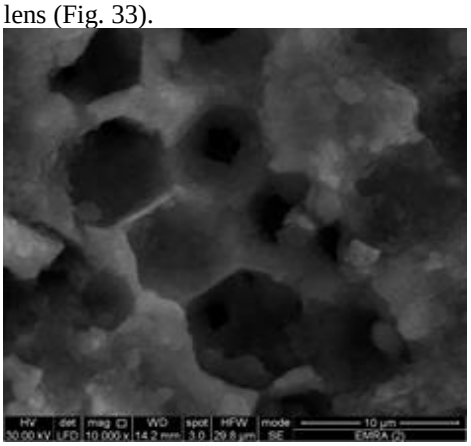

Fig. (32): *BSE image of six-sided, well crystalline kaolinite showing edge to edge interface structure. Cretaceous grey kaolin of the upper lens of Salia.*

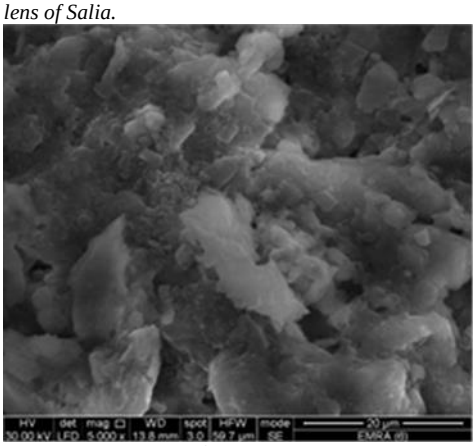

Fig. (33): *BSE image of the Cretaceous grey silty kaolin of the lower lens showing pseudo-hexagonal kaolinite crystals with few scattered quartz grains in the lower left corner of the image. Note the poly-crystalline nature and the overgrowth of quartz grains.*

4. Geochemistry of kaolin deposits

The present work discusses the diagnostic geochemical characteristics of the Lower Cretaceous sedimentary kaolin deposits under consideration. The Lower Cretaceous kaolin deposits are embedded within the sandstones of the Malha Formation.

4.1 Materials and methods

Twenty samples have been chosen for chemical analysis of the studied kaolin deposits. These samples represent the lateral and vertical variations of the encountered kaolin lenses. The Lower Cretaceous kaolin deposits were represented by twenty samples; seven samples from Shushet Abu El-Nimran, seven

samples from Rueikna, and six samples from Salia areas (Tables 1, 2 and 3). The ratio of alumina/silica and ratios between the common isovalents, such as Zr/Hf, Nb/Ta, Y/Ho and Th/U, are listed in table (4), which involves also the LREE/HREE ratio and ΣREE. The tetrad effect (t1, t3 and t4) of the REE was calculated but it is always of insignificant value.

The chemical analysis of the major, trace and rare earth elements (REE) was conducted on whole rock samples using the inductively coupled plasma-mass spectrometric analysis (ICP-MS) in the Acme lab of Vancouver in Canada (Tables 1, 2, and 3). The obtained data are used to interpret the genetic and diagenetic bearings of the studied kaolin resources.

5. Results and discussion

Based on color, the kaolin resources can be classified into two main varieties, namely; dark and bright colored. Shushet Abu El-Nimran resources are generally darker in color compared to those of the Rueikna and Salia resources. The coloring agents of the dark variety are organic matter, which renders the kaolin gray shades, and ferruginous materials. The organic matter can be destructed upon heating whereas the ferruginous material is costly to eliminate. Petrographically, the ferruginous coloring agents concentrate along lamination but may also stain the resources.

The averages of the results on the kaolin resources in Shushet Abu El-Nimran, Rueikna, and Salia are compared to available information on local and international deposits, as well as the Upper Continental Crust (Table 5). According to Baioumy and Gilg, the examined kaolin resources are slightly lower in grade than those in Kalabsha, close to Aswan (2011). Free silica appears to be the primary kaolin dilutant. The examined kaolin deposits have a greater SiO2 content than the benchmark data. Due to the large percentage of admixed silt size, the investigated kaolin has a comparatively greater content of TiO2. The alkali earth's (MgO and CaO) or even the alkali's contents (Na2O and K2O) are low when compared to the reference data. Th and U radionuclides are diagnostically elevated in the kaolin deposits under study.

The obtained data reflect a marked difference in composition between the different occurrences or even along the kaolin sedimentary sequence in the same area. The comparison between the Shushet Abu El-Nimran, Rueikna and Salia kaolin resources proposes that Shushet Abu El-Nimran kaolin deposits is considerably enriched in alkalis Na2O but depleted in CaO and MgO (Fig. 34-35). This is most likely a result of the Rueikna and Salia kaolin deposits' availability of dolomite and calcitic material. Salia kaolin resources shows enrichment in CaO and MgO while it is depleted in alkalis (Na2O and K2O) compared to Rueikna kaolin resources, which indicates more availability of dolomite and calcitic material of the former available in Rueikna kaolin resources (Fig. 36).

Table 1 Chemical analysis data of major oxides (Wt. %) of the studied kaolin

Locality		Sample No.	SiO_2	TiO_2	Al_2O_3	Fe_2O_3	MgO	CaO	Na_2O	K_2O	P_2O_5	L.O.I	Total
Shushet Abu-El Nimran	Bottom	2	63.45	2.48	24.30	0.69	0.02	0.20	0.12	0.05	0.14	8.33	99.78
		5	54.12	1.53	30.60	1.82	0.03	0.10	0.28	0.23	0.11	11.08	99.90
		6	59.91	2.48	29.55	3.70	0.03	0.10	0.08	0.06	0.13	3.93	99.97
		10	57.07	3.10	28.01	3.60	0.02	0.25	0.09	0.06	0.18	7.61	99.99
	Upper	19	60.00	2.27	28.49	1.02	0.03	0.13	0.11	0.05	0.13	7.64	99.87
		22	52.49	2.36	31.32	0.92	0.02	0.17	0.03	0.06	0.13	12.48	99.98
		25	56.47	3.00	27.40	3.09	0.03	0.11	0.11	0.05	0.16	9.55	99.97
Rueikna	Bottom	32	60.23	1.51	26.03	1.25	0.05	0.35	0.13	0.16	0.12	10.13	99.96
		35	45.60	2.08	38.17	1.81	0.06	0.09	0.01	0.26	0.15	11.74	99.97
		36	44.62	1.41	39.06	2.21	0.17	0.55	0.10	0.03	0.08	11.76	99.99
		38	57.62	3.73	26.44	1.00	0.03	0.40	0.13	0.05	0.13	10.45	99.98
	Upper	47	58.07	3.10	28.01	3.60	0.08	0.50	0.09	0.16	0.18	6.20	99.99
		51	58.37	3.00	28.61	2.00	0.08	0.55	0.09	0.11	0.18	7.00	99.99
		54	52.29	2.36	31.52	0.92	0.09	0.36	0.04	0.16	0.13	12.11	99.98
Salia	Bottom	65	60.02	2.20	28.49	1.00	0.06	0.23	0.11	0.14	0.14	7.48	99.87
		68	55.49	2.35	30.32	0.93	0.09	0.37	0.03	0.16	0.13	10.11	99.98
		70	60.00	1.26	26.26	1.50	0.05	0.35	0.13	0.16	0.12	10.13	99.96
	Upper	77	61.30	2.27	27.49	1.02	0.06	0.23	0.11	0.15	0.14	7.10	99.87
		80	45.04	2.08	38.77	1.81	0.06	0.09	0.01	0.26	0.15	11.70	99.97
		87	57.62	2.73	27.44	3.00	0.03	0.40	0.13	0.05	0.13	8.45	99.98

Table 2 Chemical analysis data of trace elements (ppm) of the studied kaolin

Locality		Sample No.	Be	Cs	Rb	Sr	V	Co	Sn	Ga	W	Zr	Hf	Nb	Ta	Th	U
Shushet Abu-El Nimran	Bottom	2	4	<0.1	0.2	114	104	3.9	9	47.2	3	781	17.6	94	5.6	12.6	3.4
		5	3	<0.1	0.2	140	136	7.8	7	52.6	2.3	712	15.8	102	6.5	19	3.5
		6	1	<0.1	0.2	89	206	10.3	12	53.4	4.5	1066	25.9	152	9.2	23	5.7
		10	1	<0.1	0.2	92	209	10.1	10	52.1	4.4	720	21.2	122	7.1	20	3.8
	Upper	19	2	0.2	3.5	155	114	3.9	5	40.7	1.7	512	11.9	74	5	17.6	4.2
		22	4	0.5	2.6	187	151	6.9	7	40.1	2	606	13.3	83	5	15.7	3.9
		25	<1	0.2	2	210	151	2.9	5	33.9	2.1	652	15.4	76	4.7	14.6	3.6
Rueikna	Bottom	32	2	0.1	1.1	160	121	3.7	6	41.1	2	641	16.1	81	5.4	17.3	4
		35	4	<0.1	2.2	137	102	3.7	7	27.1	2.4	586	13.9	90	5.3	18.2	4.2
		36	4	<0.1	0.4	113	146	4.5	7	41.8	1.4	627	14.7	77	4.9	10	2.8
		38	3	<0.1	1.2	238	122	4.2	6	51.9	1.3	572	14.2	89	6	18.5	4.6
	Upper	47	1	<0.1	4.6	156	168	2.1	5	45.6	2.4	672	15.4	69	4.3	17.9	4
		51	5	0.2	1.5	180	206	2.6	6	45.7	1.9	680	15.8	86	5.5	20	3.9
		54	2	0.1	0.7	162	130	2.7	6	41.7	1.9	574	14.4	90	6.1	18.1	5
Salia	Bottom	65	2	0.2	3.4	156	115	3.8	5	40.8	1.8	513	12.1	75	5.1	17.7	4.3
		68	4	0.5	2.5	188	152	6.7	7	40.2	2.1	608	13.4	84	5.2	15.8	4.1
		70	<1	0.2	2.1	212	153	2.8	5	34.1	2.2	654	15.5	77	4.8	14.8	3.7
	Upper	77	2	0.1	1.2	161	123	3.8	6	41.2	2.1	642	16.2	82	5.5	17.4	4.1
		80	4	<0.1	2.3	164	124	3.8	7	45.8	2.5	681	16.1	92	5.4	18.1	4.1
		87	4	<0.1	1.3	157	169	4.6	7	52.1	1.5	575	14.5	90	6.1	18.6	4.7

Table 3 Chemical analysis data of the rare earth elements of the studied kaolin

Locality		Sample No.	Y	La	Ce	Pr	Nd	Sm	Eu	Gd	Tb	Dy	Ho	Er	Tm	Yb	Lu
Shushet Abu-El Nimran	Bottom	2	40.3	61.5	116.4	11.37	35.1	6.26	1.32	6.42	1.03	7.19	1.37	4.25	0.64	4.47	0.68
		5	45.5	64.7	117.4	12.88	44.8	7.93	1.74	7.72	1.23	8.26	1.6	4.8	0.7	4.69	0.7
		6	56.6	37.9	67.3	6.99	22.1	5.04	1.29	6.7	1.31	9.09	2.03	6.21	0.95	6.31	1.03
		10	55.2	37	66.3	6.02	21.2	5.02	1.27	6.5	1.21	9.06	2.01	6.11	0.85	6.21	1.01
	Upper	19	45.5	84.3	157.4	16.57	57.6	9.54	2.03	8.13	1.28	8.12	1.59	5	0.71	4.19	0.68
		22	48.7	60.9	125.2	13.68	50.6	9.9	2.25	9.09	1.41	8.94	1.72	5.19	0.76	5.07	0.74
		25	43.7	89.6	194.7	20.45	72.6	13.62	2.81	10.23	1.43	8.96	1.62	4.57	0.72	4.66	0.73
Rueikna	Bottom	32	40.8	96.6	193.8	20.35	62.3	9.85	1.9	7.85	1.19	7.83	1.49	4.66	0.67	4.47	0.7
		35	32.8	36.9	191.8	20.84	58.4	8.92	1.78	8.23	1.25	8.27	1.12	4.84	0.7	4.94	0.69
		36	50.4	87	104.7	8.94	37.8	7.01	1.55	6.8	1.22	8.86	1.79	5.26	0.83	5.64	0.8
		38	50.2	62.5	119.9	11.22	37.5	6.98	1.25	6.9	1.12	8.75	1.52	5.11	0.73	5.22	0.75
	Upper	47	43.7	60.1	168.9	17.54	34	7.05	1.47	6.67	0.96	5.7	1.56	3.39	0.52	3.46	0.51
		51	43.9	82.9	104.2	11.52	80	16.67	3.46	14.38	2.12	12.51	1.58	6.56	1	6.16	0.9
		54	60.6	62.9	77.5	12.47	46.6	11.39	2.49	10.32	1.41	9.1	2.27	4.92	0.73	4.7	0.72
Salia	Bottom	65	45.1	83.3	156.4	16.47	57.1	9.75	2.13	9.13	1.3	8.1	1.61	5.1	0.7	4.21	0.65
		68	48.2	60.1	125.1	13.54	50.3	9.72	2.26	9.1	1.31	8.83	1.69	5.2	0.75	5.16	0.72
		70	43.1	89.2	194.4	20.52	72.2	13.54	2.61	10.4	1.4	8.75	1.6	4.61	0.71	4.72	0.71
	Upper	77	40.5	96.1	193.6	20.26	62.6	9.21	1.85	7.55	1.2	7.8	1.5	4.65	0.68	4.52	0.7
		80	43.6	82.6	168.5	17.74	58.1	8.71	1.71	8.13	1.24	8.25	1.61	4.85	0.71	4.99	0.71
		87	50.1	62.4	104.3	11.45	37.2	7.05	1.45	6.6	1.21	8.82	1.81	5.2	0.84	5.7	0.8

Table 4 Important ratios of alumina/silica, common isovalents and total REE in the studied kaolin

Locality		Sample No.	Al_2O_3/ SiO_2	Zr/Hf	Nb/Ta	Y/Ho	Th/U	LREE/ HREE	Total REE
Shushet Abu-El Nimran	Bottom	2	0.4	44.37	16.78	29.41	3.7	8.42	258
		5	0.6	45.06	15.69	28.43	5.42	8.17	279.15
		6	0.5	41.15	16.52	27.88	4.03	4.21	174.25
		10	0.5	33.96	17.18	27.46	5.26	4.18	169.77
	Upper	19	0.5	43.02	14.8	28.61	4.19	10.57	357.14
		22	0.6	45.56	16.6	28.31	4.02	7.72	295.45
		25	0.5	42.33	16.17	26.97	4.05	11.3	426.7
Rueikna	Bottom	32	0.4	39.81	15	27.38	4.32	12.76	413.66
		35	0.8	42.15	16.98	29.28	4.33	9.95	348.68
		36	0.9	42.65	15.71	28.15	3.57	7.49	278.2
		38	0.4	40.28	14.83	33.02	4.02	7.59	269.45
	Upper	47	0.5	43.63	16.04	28.01	4.47	11.86	311.83
		51	0.5	43.03	15.63	27.78	5.12	6.06	343.96
		54	0.6	39.86	14.75	26.69	3.62	5.75	247.52
Salia	Bottom	65	0.5	42.39	14.7	28.01	4.11	10.15	355.95
		68	0.5	45.37	16.15	28.52	3.85	7.71	293.78
		70	0.4	42.19	16.04	26.93	4	11.34	425.37
	Upper	77	0.4	39.62	14.9	27	4.24	12.84	412.22
		80	0.9	42.29	17.03	27.08	4.41	10.72	367.85
		87	0.5	39.65	14.75	27.67	3.95	7.1	254.83

Table 5 Averages of the present work compared with published data and Upper Continental Crust

Oxides% or Elements ppm	Present work (Sinai Kaolin)			Aswan kaolin	Turkey kaolin	Bostwana Kaol. U. Conti. Crust.	
	Shushet Abu El-Nimran (n=7)	Rueikna (n=7)	Salia (n=6)	Baioumy & Glig (2011)	Karakaya (2009)	Ekosse (2001)	Rundnick & Gao (2010)
SiO_2	57.64	53.82	56.57	45.13	45.9	45.34	66.60
TiO_2	2.46	2.45	2.14	2.11	NA*	0.68	0.64
Al_2O_3	28.52	31.12	29.79	35.29	34.60	28.57	15.40
Fe_2O_3	1.69	1.68	1.54	3.05	1.06	2.65	5.04
MgO	0.02	0.08	0.06	0.28	0.23	1.06	2.48
CaO	0.15	0.40	0.28	0.12	0.40	0.08	3.59
Na_2O	0.12	0.08	0.09	0.16	0.15	0.23	3.27
K_2O	0.08	0.13	0.15	0.02	0.27	3.87	2.80
P_2O_5	0.14	0.14	0.13	0.10	0.12	0.06	0.15
L.O.I	9.09	10.05	9.16	12.90	16.93	12.28	NA
Rb	1.27	1.67	2.13	NA	15.4	119	84
Sr	141	163	173	49	372	136	320
V	153	142	139	763	80	229	97
Co	6.5	3.3	4.2	4.5	2.2	50	17.3
Ga	45.7	42.1	42.4	NA	22	NA	17.5

Zr	721	621	612	1413	111	240	193
Hf	17.3	14.9	14.6	NA	6.3	NA	5.3
Nb	100	83	83	92	6.2	17	12
Ta	6.1	5.3	5.3	NA	0.5	NA	0.9
Th	17.5	17.1	17	NA	7.3	14	10.5
U	4	4	4.1	NA	1.9	NA	2.7
Y	47	46	45	108	14	22	21
∑REE	280	316	351	334	138	NA	148

NA* Means not analyzed

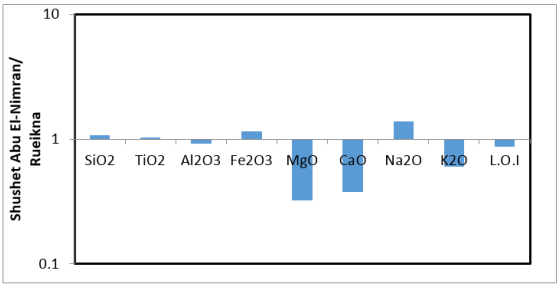

Fig. (34): Average of major oxides of the studied Shushet Abu El-Nimran kaolin deposits normalized to the average Rueikna kaolin deposits.

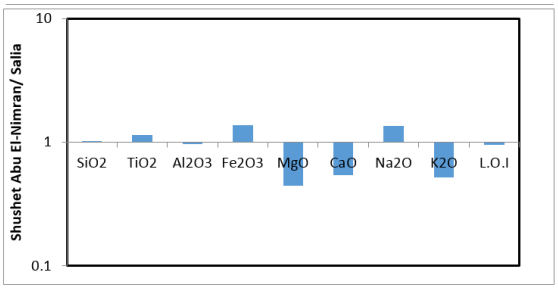

Fig. (35) : Average of major oxides of the studied Shushet Abu El-Nimran kaolin deposits normalized to the average Salia kaolin deposits

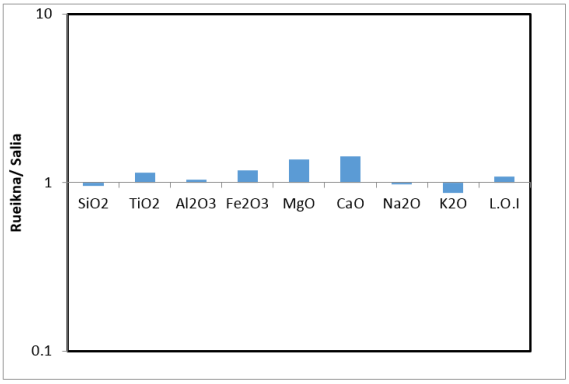

Fig. (36): Average of major oxides of the studied Rueikna kaolin deposits normalized to the average Salia kaolin deposits

The Rueikna and Salia kaolin deposits with regard to trace elements exhibit considerable enrichment in Rb , which can be viewed as a direct feedback for the substantial rise in K2O. Shushet Abu El-Nimran kaolin is enriched in V, Co, Ga, Zr, Hf, Nb, Ta, Th and Y but slightly depleted in U and depleted in REE (Fig. 37-39).

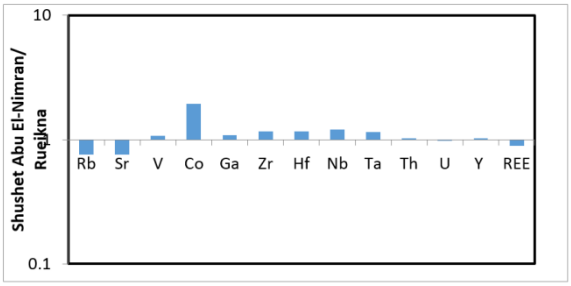

Fig. (37): Trace elements average of the studied Shushet Abu El-Nimran kaolin deposits normalized to the average Rueikna kaolin deposits.

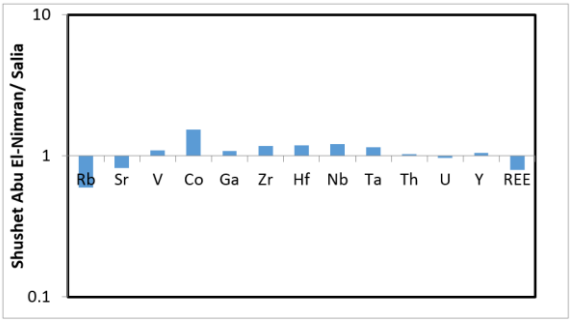

Fig. (38): Trace elements average of the studied Shushet Abu El-Nimran kaolin deposits normalized to the average Salia kaolin deposits

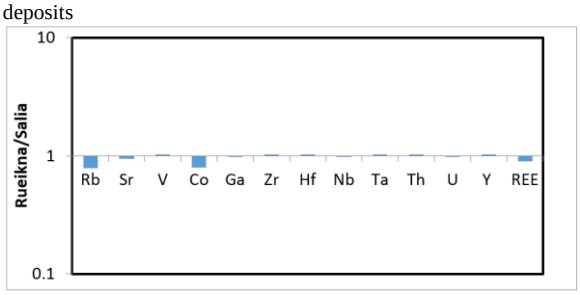

Fig. (39): Trace elements average of the studied Rueikna kaolin deposits normalized to the average Salia kaolin deposits

The examined kaolin deposits show a relative enrichment in silica at the expense of alumina when compared to high quality kaolin from Georgia in the United States (Murray, 1961) and West Cameroon (Tassongwa et al., 2014), except samples number 36 of Rueikna kaolin deposit and 80 of Salia kaolin deposit.

5.1 Kaolin versus quartz:

The examined Lower Cretaceous kaolin deposits of Shushet Abu El-Nimran, Rueikna, and Salia are rich in large-sized detrital quartz from a petrographic perspective. However, the proportion of the well-developed kaolinite flakes and the detrital admixture varies from lens to lens. This likely denotes differences in subaerial and weathering activity, as well as paleo-currents. Since alumina and silica have a negative relationship, free-silica appears to be the principal kaolin grade diluent (Fig. 40).

The highest grade of the investigated kaolin, sample number 80 (upper lens of Salia), has a Si/Al molecular ratio of one, which indicates an almost complete absence of detrital quartz. In contrast, sample number 2 (bottom lens of Shusha), the lowest grade of kaolin, shows a Si/Al molecular ratio of 2.6, where free silica predominates over kaolin. This sample also has the lowest amount of alumina (24.3%).

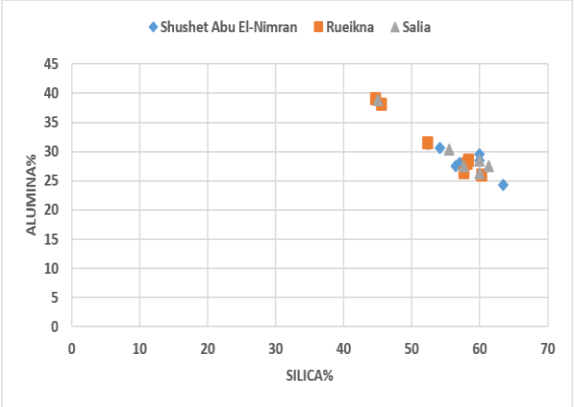

Fig. (40): Opposite relationship between silica and alumina of the studied kaolin

5.2 Chemical weathering index:

Chemical index of alteration (CIA) is the most reliable index for measuring intensity of weathering in the sedimentary environments. It was proposed by Nesbitt and Young (1982), according to the equation; $CIA=(Al_2O_3/Al_2O_3+Na_2O+K_2O+CaO)*100$ assuming that chemical weathering leads to mobilization of alkalis and CaO from silicate minerals relative to the immobile alumina. According to Fedo *et al.*, (1995), the CaO in the above equation represents only CaO in the feldspar lattice and not that in carbonate phases. The examined kaolin deposits have CIA values between 97.4 and 99.2, which indicates that chemical weathering has vast limits (Fig. 41).

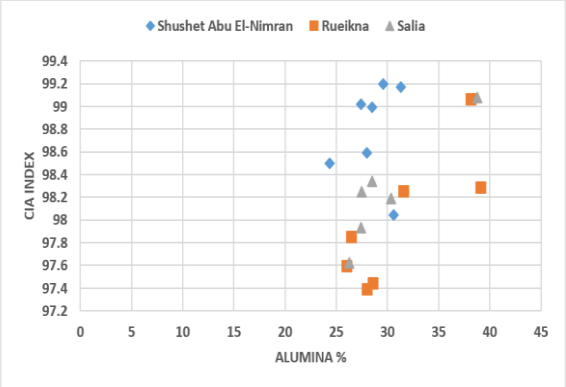

Fig. (41): Relationship between CIA and alumina as a measure of kaolin grade

The diagram above demonstrates that as the CIA index rises, so does the quality of the kaolin deposits. The kaolin deposits are concentrated in the low magnesia and medium potash fields in the relation of magnesia versus potash plots, which could be because illite and chlorite minerals aren't present there (Fig. 42).

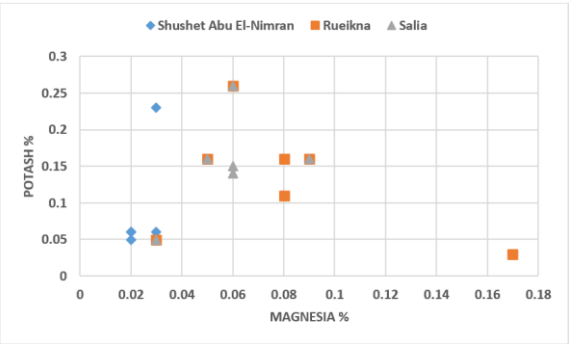

Fig. (42): Magnesia versus potash relation showing the low magnesia, medium potash field of most samples of kaolin deposits of the study areas

5.3 Shushet Abu El-Nimran versus Rueikna and Salia kaolin:

The examined kaolin resources from Shushet Abu El-Nimran and those from the Rueikna and Salia regions differ in terms of the abundance and distribution of the major and trace elements. Additionally, variations between upper and lower lenses of the same age and occurrence are noted. Both genetic and diagnostic factors can be linked to changes in chemical composition.

An accurate indicator of the kaolin grade is the Al2O3/SiO2 ratio. For the Shushet Abu El-Nimran resources, which comprise between 52.49 and 63.45% SiO2 and between 24.30 and 31.32% Al2O3, this ratio varies between 0.4 and 0.6. (Table 1). For the Rueikna kaolin, which includes between 44.62 and 60.23% SiO2 and 26.03 and 39.06% Al2O3, the ratio fluctuates between 0.4 and 0.9. (Table 1). The ratio for Salia kaolin, which comprises between 45.04 and 61.30% SiO2 and 26.26 and 38.77% Al2O3, ranges from 0.4 to 0.9. (Table1). Currently, the Rueikna and

Salia kaolin deposits, which have the highest kaolin content, are the only mineable Cretaceous kaolin resources, while Shushet Abu El-Nimran kaolin resources is of lower quality than the other study areas, it is economic in zeolite synthesis as it has kaolin of dark dry color and high LOI % ranging from 6.93 – 12.48 % which indicates that it contains a high percentage of organic matter and after curing the kaolin at 700 °C and removing the organic matter, the kaolin will be turned into metakaolin and the Al_2O_3 % will increase, hence the kaolin will be economic only in industries that requires curing the kaolin before usage such as zeolite synthesis (Table 1).

5.4 Trace elements:

The present discussion on the trace elements is based on data of 15 trace elements in the studied whole kaolin deposits (Table 2). These trace elements include alkalis (Rb and Cs), alkali earths (Be and Sr), heavy metals (V, Co and Sn), high field strength elements (Zr, Hf, Nb, Ta and W), and radionuclides (Th and U). The REE geochemistry is discussed hereafter under separate headline.

The comparison between the kaolin deposits of study areas points to the marked enrichment of Rueikna and Salia in Rb, as an immediate response to the high K_2O, as well as moderate enrichment in Sr and U in addition to REE. The lower lens of the Salia region is where this enrichment in Rb is most readily apparent. Co is considerably enriched in the Shushet Abu El-Nimran deposits, while the high field strength elements have only slightly increased (Fig. 43). For the pisolitic kaolin deposits of Kalabsha, close to Aswan, Egypt, Baioumy and Gilg (2011) found strikingly high average concentrations of Zr (1413 ppm) and V (763 ppm).

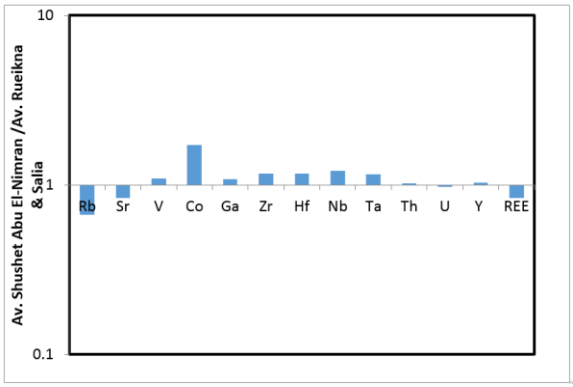

Fig. (43): Average trace elements composition of Shushet Abu El-Nimran kaolin normalized to that of the average Rueikna and Salia kaolin

According to Lopez, et al. (2005), the high field strength elements (HFSE) are most abundant in silts, indicating that accessory minerals like zircon and Nb-bearing phases are mostly concentrated in silt lithology. The most accurate chondritic ratios for Zr/Hf and Nb/Ta, respectively, are 34.2 0.3 and 17.6 1, according to Weyer et al., 2002. The Nb/Ta geochemical pair, which has values slightly lower (16 on average) than the chondritic pair, appears to be extremely constant (Fig. 44). There is consistency across the kaolin deposits in the research locations despite the strong link between Zr and its heavier isovalent (Hf). For the studied locations, the typical Zr/Hf ratio is 42. (Fig. 45). The high Zr/Hf ratio may indicate origin from a differentiated provenance while both Zr and Hf are partners of zircon, which is the detrital mineral proper.

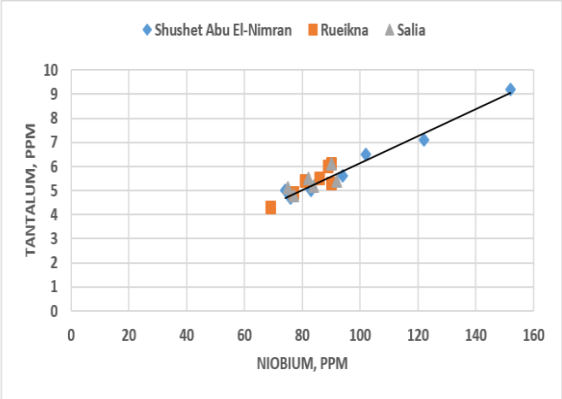

Fig. (44): Perfect coherence between Nb and Ta in the studied kaolin deposits

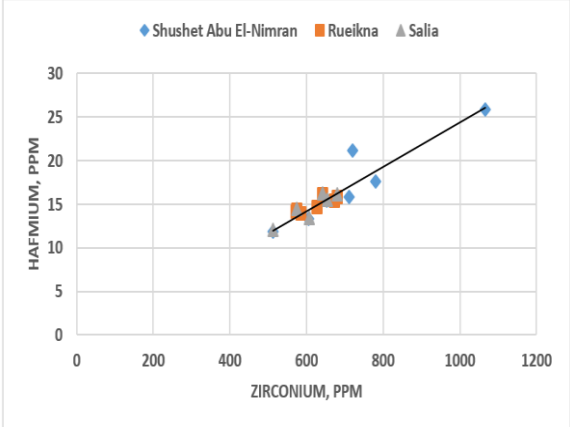

Fig. (45): Perfect coherence between Zr and Hf in the studied kaolin deposits

For all of the examined samples, the Y/Ho ratio is quite close to the chondritic value (28). The Th/U ratio, on the other hand, exhibits distinct differentiation and a common state of disequilibrium. Th content (10 to 23 ppm) always outweighs U content in these situations (2.8 to 5.7 ppm). For the kaolin deposits in the research area, the Th/U ratio is non-CHARAC (charge and radius control), and it ranges from 3.6 to 5.5. (Fig. 46).

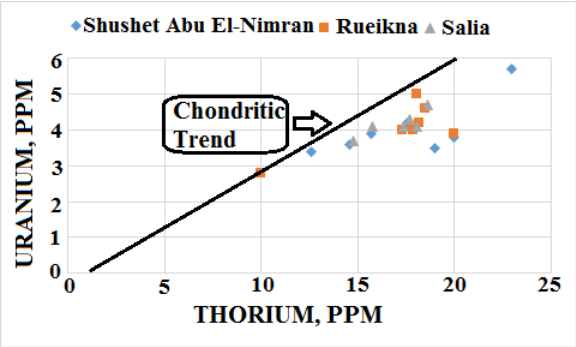

Fig. 46: *Plot of thorium versus uranium, showing the non-CHARAC behavior of the studied kaolin deposits*

Because the TH/U ratio is less than the chondritic (CHARAC) value (2.8), it is possible that U has been mobilised from the kaolin deposits. Th persists in the tetravalent immobile state while U oxidises into its hexavalent mobile state under the prevalent exogenic conditions. The research locations' kaolin samples exhibit a pronounced decrease of U in comparison to Th. The U must have been mobilised during the pluvial times.

5.5 Rare earth elements (REE) geochemistry:

The Shushet Abu El-REE Nimran's budget typically exceeds that of the Rueikna and Salia kaolin resources. The REE content ranges from 247 to 425 ppm, with Rueikna and Salia having an average of 334 ppm. For the Shushet Abu El-Nimran kaolin deposits, the REE level ranges from 170 to 427 ppm, averaging 280 ppm. The obtained REE budget is often greater than values published for kaolin occurrences (e.g., Tassongwa, et al., 2014; and Karakaya, 2009) but low overall, close to the values quoted for the pisolitic kaolin resources of the Kalabsha area near Aswan by Baioumy and Gilg (2011).

Though, it can generally be concluded that the kaolin of the Rueikna and Salia are richer in REE relative to that of the Shushet Abu El-Nimran. The kaolin of the study areas shows intimate coherence (Fig. 47). The simple explanation for these disparities is that the LREE signature substantially imparts REE content to the research area's kaolin.

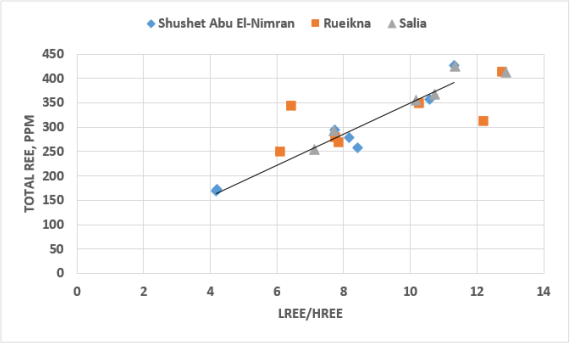

Fig. (47): Relationship between total REE content and LREE/HREE for the studied kaolin resources

Normalized REE patterns:

According to McLennan (1989) and Gromet et al. (1984), respectively, the REE concentrations of the examined kaolin resources have been standardised to chondrite and North American Shale Composite (NASC). The following significant implications are reflected by the normalisation to chondrite (Fig. 48);

1. LREE have wider variation than HREE for the study areas of kaolin.
2. Eu negative anomaly in the studied kaolin samples.
3 .Despite being deposited under pluvial conditions, none of the examined kaolin deposits exhibit Ce anomaly.
3. For the examined kaolin, the slope of the patterns shows a larger prevalence of the LREE over the HREE.

4.

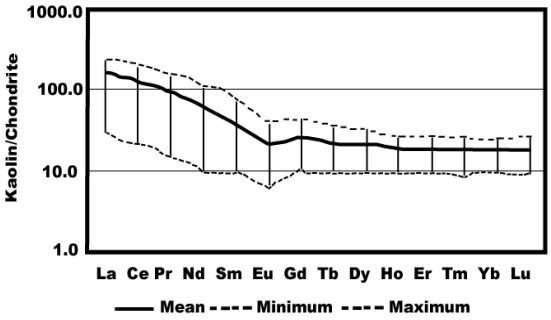

Fig. (48): Chondrite-normalized REE patterns of the studied kaolin resources

REE distribution in different kaolin lenses:

Impregnation of the upper boundary of the kaolin lenses at contact with the hosting sandstones by supergene meteoric water carrying iron oxy-hydroxides (ferrugination) is customarily accompanied by decline in the REE budget. Low REE contents of 255, 174 and 170 ppm have been recorded for the kaolin on boundaries with the ferruginated kaolin lenses; Upper Salia and Lower Shushet Abu El-Nimran area, respectively. However, this observation is not consistent, since the ferruginated upper surface of bottom lens at Salia area, display marked enrichment in REE, up to 425 ppm, whereas the non-ferruginated part of this bed is depleted in REE (293 ppm). This is in line with Awwiller's (1994) conclusion that there was little proof of REE redistribution beyond the local level. While there is some evidence that fractionation between the HREE and LREE can occur during authigenic mineral growth, REE mobility during diagenesis has also been observed within sandstones of the European continental shelf, associated with the growth of authigenic francolite (e.g., Bouch et al., 1995). However, the author thinks that the intensity and strength of the water paleo-currents involved in the deposition of each lens determine the REE concentrations.

The upper kaolin lens of the Shushet Abu El-Nimran deposit, where the content ranges from 295 to 427 ppm, has the greatest REE budget (Table 3). The highest SiO2, Zr, and Th concentrations, which are often regarded as terrestrial indicators, are present along with these high REE values. This can be held as evidence for the detrital origin of the REE. The highest REE concentration recorded in the study areas kaolin deposits is 427 ppm in the commercial kaolin grade of Upper Shusha kaolin lens while the highest REE in commercial kaolin of Lower lens at Salia area is 425 ppm and 413 ppm at lower Rueikna kaolin lens. In fact, there is no intimate coherence between the REE content and both major or trace elements in the kaolin resources.

6.Possible Applications

6.1 Papermaking industry

This sector needs kaolin that is of the highest quality possible since it gives paper its topographically flat, bright surface, good ink receptive characteristics, and good opacity. Additionally, kaolin has rheological characteristics that are appropriate for high-speed paper coating in the present era (Manju, 2002). (table. 6). Fine, white pigment powders used as paper fillers are chemically or directly derived from natural minerals. Fillers are used to close up gaps between fibres. Kaolin, precipitated calcium carbonate, powdered calcium carbonate, talc, gypsum, titanium dioxide, and synthetic silicates are a few of the important fillers used in the production of paper (Rajala, 2012). The kaolin samples gathered from the research locations can't be used internationally in the paper producing sector due to their poor brightness% compared to these typical kaolin qualities. They range in colour from light to dark grey due to contamination by TiO2, organic matter, or yellowish to reddish colours due to staining by ferruginous materials, which can be seen even with the naked eye. It is less expensive to import white kaolin with high brightness than to beneficiate the kaolin from the study areas since it can be used after an expensive beneficiation procedure.

Table. 6: Typical properties of filling and coating kaolin according to Manju, (2002)

Property	Coating clay	Filler clay
% Brightness (International Standards Organization)	81.5 – 90.5	76 – 82
% Yellowness	4 – 6.5	5.7 – 8
Particle size % <2µm > 10 µm > 53 µm	 75 – 95 0 – 6 0.02 max	 25 – 60 6 – 25 0.05 max
Viscosity concentration (% solids at 5 poise, at 22°C)	64.2 – 74.5	61. 2 – 71.5

6.2 Refractory manufacturing

Refractories are non-metallic building materials that can withstand high temperatures and are appropriate for use in industrial furnaces. Their principal use is because to their resistance to high temperatures, but they frequently need to endure abrasion, load, slag/molten metal, salt, and one or more of the following harmful processes. To create a refractory lining, kaolin clay is roasted at 1200°C for 8 hours, combined with various amounts of raw kaolin, and then correctly formed into briquettes using potter's clay with sufficient plasticity as a binder (Aramide and Seidu, 2013). The kaolin samples obtained from the study areas can't be utilised in the global market to manufacture refractories because all samples collected had low Al2O3% (ranging from 24.3 to 39.06%) compared to the ideal kaolin used in the global market to manufacture refractories (39.69%, Al2O3). On the local market, grade 1 kaolin (Al2O3 is greater than 33%) can be utilised in the production of refractory materials. Al2O3 is present in samples from the upper Salia and bottom Rueikna kaolin lenses with corresponding concentrations of 39.06 and 38.77%. These lenses also have minor levels of radioactivity and oxides of iron, magnesium, calcium, sodium, and potassium. As a result, it qualifies for the refractory industry on the local market but is unable to compete on the global market.

Table 7: *Chemical composition of the ideal kaolin used in refractory industry, according to Aramide and Seidu, 2013.*

Sample	Raw Kaolin
SiO_2 (%)	42.78
Al_2O_3 (%)	39.69
Fe_2O_3 (%)	1.26
TiO_2 (%)	1.30
CaO (%)	0.18
MgO (%)	0.18
Na_2O (%)	0.02
K_2O (%)	0.07
LOI (%)	14.10

6.3 Ceramic Manufacturing

The grade needed for kaolin depends on the use because it is used for many different things. Despite the fact that the paper sector consumes the most kaolin (as filler). It is most frequently utilised as a conventional raw material in the ceramic industry. In addition, kaolin is utilised as a filler in the manufacture of synthetic zeolites,

refractory materials, rubber, plastics, pigments, cosmetics, pharmaceuticals, and food products. Because it affects how ceramic masses behave following heat treatment, kaolin's chemical composition is significant; an Al2O3 percentage of greater than 30% is required to increase refractory and mechanical resistance (Benea and Gorea, 2004). In contrast to the typical kaolin characteristics (table 8), some of the kaolin samples gathered from the research locations can be employed in the production of ceramics on the international market. Al2O3 is present in samples from the kaolin lenses in the lower Rueikna and upper Salia with respective concentrations of 39.06 and 38.77%. These samples also exhibit low radioactivity, allowing them to be exported and to compete in both the domestic and international markets for the production of ceramics. In contrast to the ideal kaolin utilised in ceramic manufacturing, the examined kaolin samples are often low in alkali, earth alkalis, and silica but higher in Fe2O3 and TiO2. As a result, it is advised to treat kaolin before export by washing it with water first, then adding H2SO4 to remove any excess Fe2O3, which is the easiest and most affordable method available. Grade 2 kaolin with an Al2O3% content of between 30 and 33% is needed for the local market. Therefore, it is advised to use kaolin from all of the studied locations in domestic ceramic manufacturing.

Table 8: *Chemical composition of the ideal kaolin used in ceramic industry according to Benea and Gorea, (2004)*[*]

Oxides %	Ideal Kaolin[*]
SiO_2 (%)	49.55
Al_2O_3 (%)	35.38
Fe_2O_3 (%)	0.90
TiO_2 (%)	0.41
CaO (%)	0.24
MgO (%)	0.32
K_2O (%)	1.06
LOI (%)	12.15

7.Conclusion

Kaolin deposits in SW Sinai represented one of the most important reserve that would be used in traditional and modern industrial purposes.

But according to the XRD examination of the kaolin under study, kaolinite is the primary component and is occasionally joined by dickite, illite, smectite, and halloysite. Along with minor amounts of gypsum and dolomite, weak diffractions associated with hematite, and the accessory mineral monazite, quartz is the major non-clay mineral. Ferrugination typically occurs near the upper limits of the kaolin lenses where it comes into touch with the sandstone strata below, which may be a sign of supergene activity. Different amounts of organic content, major clay-size fractions (> 75%, by volume), detrital quartz grains (5 to 25%), and levels of ferrugination are present in the investigated kaolin. These characteristics influence the kaolin deposits under study's colour and compactness. Additionally, the high Al2O3/SiO2 ratio of 0.53 reveals the superior quality of Sinai's Cretaceous kaolin deposits. Si/Al molecular ratio of 0.9 indicates a high grade of kaolin in the upper lens in Salia and lower lens in Rueikna, respectively. The Rueikna and Salia kaolin deposits in Rb exhibit considerable enrichment in the comparison with regard to trace elements, which can be viewed as a direct feedback for the pronounced rise in K2O. Shushet Abu El-Nimran kaolin is slightly depleted in U and depleted in REE but enriched in V, Co, Ga, Zr, Hf, Nb, Ta, and Y. A greater input of LREE is a characteristic of the Cretaceous kaolin (Monazite signature). Because the TH/U ratio is less than the chondritic (CHARAC) value (2.8), it is possible that U has been mobilised from the kaolin deposits. Th persists in the tetravalent immobile state while U oxidises into its hexavalent mobile state under the prevalent exogenic conditions. The research locations' kaolin samples exhibit a pronounced decrease of U in comparison to Th. The U must have been mobilised during the pluvial times. None of the examined kaolin deposits exhibits Ce anomaly, despite the very high CIA index (97.4 and 99.2), showing vast limitations of chemical weathering.

Comparatively speaking, the kaolin from the Rueikna and Salia is richer in REE than that from the Shushet Abu El-Nimran. The research areas' kaolin exhibits close coherence. The simple explanation for these disparities is that the LREE signature substantially imparts REE content to the research area's kaolin. The upper kaolin lens of the Shushet Abu El-Nimran deposit, where the content ranges from 295 to 427 ppm, has the greatest REE budget. The highest SiO2, Zr, and Th concentrations, which are often regarded as terrestrial indicators, are present along with these high REE values. This supports the idea that the REE is detrital in origin. The research area's commercial grade Upper Shusha kaolin lens has the highest REE content, at 427 ppm, while the commercial grade Lower lens in the Salia area has the highest REE concentration, at 425 ppm, and the lower Rueikna kaolin lens has the lowest REE concentration, at 413

ppm. In actuality, neither the major nor trace elements in the kaolin resources nor the REE content exhibit any close coherence.

The kaolin in the research areas does not meet the requirements for the production of refractories and papermaking sectors, although expensive beneficiation may be necessary before usage on a domestic or international scale. On the local market, grade 1 kaolin (Al2O3 is greater than 33%) can be utilised in the production of refractory materials. Some lenses also feature a modest level of radioactivity and oxides of iron, magnesium, calcium, sodium, and potassium. As a result, they are suitable for the local refractory market but probably aren't able to compete there. The high-grade kaolin from the studied areas satisfies the standards necessary for the manufacture of ceramics, allowing it to be exported and compete on both the domestic and international markets of ceramic manufacturing. In contrast to the ideal kaolin utilised in ceramic manufacturing, the examined kaolin samples are often low in alkali, earth alkalis, and silica but higher in Fe2O3 and TiO2. Because this is the cheapest and most straightforward method currently being utilised, it is advised to benefitate kaolin before export by simply washing with water and then adding H2SO4 to remove the excess Fe2O3. Grade 2 kaolin with an Al2O3% content of between 30 and 33% is needed for the local market. Kaolin can therefore be used and is advised for domestic ceramic manufacture throughout all study areas.

8.Acknowledgment

Last, we would like to pay our gratitude and our respects to our co-organizer and colleague, Prof. Dr. Ahmed El-Kammar. After helping to initiate and organize this work, Prof.Dr. Ahmed El-Kammar passed away in August of 2020. He was a dedicated professor in the Department of Geology at Cairo University in Egypt. This work could not have been done without his constant support.

9.Conflicts of interest

There are no conflicts to declare.

10.References

[1]Ababneh, A., Matalkah, F. and Aqel, R., 2020, Synthesis of kaolin-based alkali-activated cement: carbon footprint, cost and energy assessment. *Journal of Materials Research and Technology*, 9(4), 8367-8378.

[2]AbdAllah, A., 2019, Impacts of kaolin and pinoline foliar application on growth, yield and water use efficiency of tomato (Solanum Iycopersicum L.) grown under water deficit: A comparative study. *Journal of the Saudi Society of Agricultural Sciences*, 256-268.

[3]Abdallah, A.M., Adindani, A., 1963, Stratigraphy of Lower Mesozoic rocks, western side of Gulf of Suez. *Egyptian Geological Survey*, paper 27: 1-23.

[4]Abu-Zied, R.H., 2008, Lithostratigraphy and biostratigraphy of some Lower Cretaceous outcrops from Northorn Sinai, Egypt. *Cretaceous Research*, 29, 603-624.

[5]Aramide and Seidu, 2013, Production of refractory lining for diesel fired rotary furnace, from locally sourced kaolin and potter's clay. *Journal of Minerals Charac. and Eng.* 75 pp.

[6]Awad, H. M., 1995, Petrological studies on pre-Cenomanian kaolin-bearing succession at Wadi Gharandel area, Sinai. *M. Sc. Thesis Fac. Sci., Cairo Univ*., 88 p.

[7]Awwiller, D.N., 1994, Geochronology and mass-transfer in Gulf coast mudrocks (South-Central Texas, U.S.A): Rb-Sr, Sm-Nd and REE systematic. Chem. Geol., 116, 61-84.

[8]Baioumy,H. and Gilg, H.A., 2011, Pisolitic flint kaolin from Kalabsha, Egypt: A laterite-derived facies. *Sedimentary Geology*, 236, 141-152.

[9]Benea, M., Gorea, M., 2004, Mineralogy and technological properties of some kaolin types used in the ceramic industry. *Studia Universitatis Babes-Bolyai, Geologia*, 33, 37.

[10]Bloodworth, A.J., Highley, D.E., Mitchell, C.J., 1993, Industrial Minerals Laboratory Manual: Kaolin. *BGS Technical Report* WG/93/1, 76 pp.

[11]Bouch, J.E., Hole, M.J., Trewin, N.H. and Morton, A.C., 1995, Low temperature aqueous mobility of the rare earth elements during sandstone diagenesis. J. Geol. Soc. London, 152, 895-898.

[12]Boulis, S.N. and Attia, A.K.M., 1994, Mineralogical and chemical composition of Carboniferous and Cretaceous kaolins from a number of localities in Egypt. *Proc. 1st Inter. Sympo. on Industrial Applications of Clays, Cairo*, pp.99-127.

[13]Bukalo, N., Ekosse, G.I., Odiyo, J. and Ogola, J., 2019, Paleoclimatic implications of hydrogen and oxygen isotopic compositions of Cretaceous-Tertiary kaolins in the Douala Sub-Basin, Cameroon, *Comptes Rendus Geoscience*, 17-26.

[14]Cases, J.M., Liétard, O., Yvon, J., Delon, J.F., 1982, Etude des propriétés cristallochimiques,morphologiques et superficielles de kaolinites désordonnées. *Bulletin de Minéralogie* 105, 439–457.

[15]Cases, J.M., Cunin, P., Grillet, Y., Poinsignon, C., Yvon, J., 1986, Methods of analyzing morphology of kaolinite: relation between crystallographic and morphological properties. *Clay Minerals* 21, 55–68.

[16]Chargui, F., Hamidouche, M., Belhouchet, H., Jorand, Y., Doufnoune, R. and Fantozzi, G., 2018, Mullite fabrication from natural kaolin and aluminum slag. *Ceramica y Vidrio*, 57, 169-177.

[17]CIREP, 2003, Final report [by the Cosmetic Ingredient Review Panel] on the safety of aluminium silicate, calcium silicate, magnesium aluminium silicate, magnesium silicate, magnesium trisilicate, sodium magnesium silicate, zirconium silicate, attapulgite, bentonite,Fuller's earth, hectorite, kaolin, lithium magnesium silicate, lithium magnesium sodium silicate, montmorillonite, pyrophyllite, and zeolite. Int J Toxicol, 22 (Suppl 1): 37–122.
[18]Ekosse, G., 2000, The Makoro kaolin deposit, Sourtheastern Botswana: its genesis and possible industrial applications, *Applied Clay Science*, 16, 301-320.
[19]El-Kammar, A., Abu-Zied, H.T., Galal, M. and Osman, D., 2017, Composition, radioactivity, and possible applications of kaolin deposits of Sinai, Egypt. *Arab Journal of Geosciences.* 462-481.
[20]Fedo, C.M., Nesbitt, H.W. and Young, G.M., 1995, Unraveling the effects of potassium metasomatism in sedimentary rocks and paleosols, with implications for paleoweathering conditions and provenance. Geology 23, 921-924.
[21]Gámiz, E., Melgosa, M., Sánchez-Maranńön, M., Martin-Garcia, J.M., Delgado, R., 2005, Relationship between chemico-mineralogical composition and color properties in selected natural and calcined Spanish kaolins. *Applied Clay Science* 28, 269–282.
[22]Glenn, D.M., 2016, Effect of highly processed calcined kaolin residues on apple productivity and quality. *Sci.Hort*, 201, 101-108.
[23]Gromet L. P. and Dymek R. F., 1984, Nature and origin of orthopyroxene megacrysts from the St. Urbain anorthosite massif, Quebec. Can. Mineral. 22, 297-326.
[24]Hadi, E.M. and Hussein, S.I., 2019, A sustainable method for porous refractory ceramic manufacturing from kaolin by adding of burned and raw wheat straw. *Energy Proceedia*, 157, 241-253.
[25]Hafez, A.I., Gerges, N.S., Ibrahim, H.N., Abou El-magd, W.S.I and Hashem, A.I., 2017, Evaluation of kaolin clay as a natural material for transformer oil treatment to reduce the impact of ageing on copper strip. *Egyptian Journal of Petroleum*, 533-539.
[26]Hegab, O.A; Serry, M.A; Kora, M. and Abu Shabana, M., 1992, Suitability of some kaolins from West Central Sinai for use in ceramics and paper industries. *Proceeding of the Symp. held jointly with the Egyptian Geological Survey and Mining projects Authority*, 85 p.
[27]Karakaya, N., 2009, REE and HFS element behavior in the alteration facies of the Erenler Dagi volcanics (Konya, Turkey) and kaolinite occurrence, Journal of Geochemical Exploration, 101, 185-208.
[28]Lipson SM & Stotzky G., 1983, Adsorption of reovirus to clay minerals: Effects of cation exchange capacity, cation saturation, and surface area. *Applied Environmental Microbiology*, 46: 673–682.
[29]Lopez, J.M.G., Bauluz, B., Fernandez-Nieto, C., Yuste Oliete, A., 2005, Factors controlling the trace-element distribution in finegrained rocks: the Albia kaolinite-rich deposits of the Oliete Basin (NE Spain). Chemical Geology 214, 1–19.
[30]Mamudu, A., Emetere, M., Okocha, D., Taiwo, S., Ishola, F., Elehinafe, F. and Okoro, E., 2020, Parametric investigation of indigenous Nigeria mineral clay (kaolin and bentonite) as a filler in the fluid catalytic cracking unit (FCCU) of a petroleum refinery. *Alexandria Engineering Journal*, 1-10.
[31]Marfo, K.K., Arhin, D.D., Tuffou, B.A., Nyankson, E., Obada, D.O., Damoah, L.N.W., Annan, E., Yaya, A., Agyeman, B.O. and Bediako, M., 2020, The physico-mechanical influence of dehydroxylized activated local kaolin: A supplementary cementitious material for construction applications. *Case Studies in Construction Materials*, 12, e00306.
[32]Maia, A.A.B., Dias, R.N., Angelica, R.S. and Neves, R.F., 2019, Influence of an Aging Step on The Synthesis of zeolite NaA from Brazilian Amazon Kaolin Waste. Journal of Materials Research and Technology,8(3), 2924–2929 pp.
[33]Manju, C.S., 2002, Mineralogical, morphological and geochemical studies on Kundara and Madayi kaolins, Kerala. *Doctorate Thesis, University of Kerala.* 28 pp.
[34]Martin, F. , 1994, Etude cristallographique et cristallochimique de l'incorporation du germanium et du galiumdans les phyllosilicates. *Approche par synthése minéral. Thése de Doctorat, Université Aix-Marseille, France*, 200 pp.
[35]McLennan, S.M., 1989, Rare earth elements in sedimentary rocks: 1224influence of provenance and sedimentary processes. Rev. Mineral. 21, 169–200
[36]Mebrek, A., Rezzag, H., Benayache, S., Azzi, A., Taibi, Y., Ladjama, Touati, N., Grid, A. and Bouchoucha, S., 2019, Effect of chamotte on the structural and microstructural characteristics of mullite elaborated via reaction sintering of Algerian kaolin. *Journal of Materials Research and Technology*, 8(5), 4010-4018.
[37]Morsy, A.M. and Shata, S. A. A., 1992, Mineralogy and genesis of some kaolin deposits in West Central Sinai. *Proc. 3rd Conf. Geol. Sinai Develop., Ismailia*, pp. 127-140.
[38]Murray, H. H., 1961, U.S. Patent 2,995,458
Murray, H.H., 2000, Traditional and new applications for kaolin, smectite, and polygorskite: a general overview. *Applied Clay science* 17. 207-221 pp.
[39]Murray, H.H., Keller, W.D., 1993, Kaolin, kaolin and kaolin. In: Murray, H.H., Bondy, W.,Harvey, C. (Eds.), Kaolin Genesis and Utilization. Special Publication N°1, *The Clay Mineral Society*, Aurora, USA, pp. 1–24.
[40]Mustapha, S., Ndamitso, M.M., Abdulkareem, A.S., Tijani, J.O., Mohammed, A.K. and Shuaib, D.T., 2019, Potential of using kaolin as a natural adsorbent

for the removal of pollutants for tannery wastewater. *Heliyon*, 5, e02923.
[41]Nesbitt, H.W. and Young, G.M., 1982, Early Proterozoic climates and plate motions inferred from major element chemistry of lutites. Nature, 199, 715-717.
[42]Nyakairu, G.W.A., Koebrel, C., Kurzweil, H., 2001, The Buwambo kaolin deposit in central Uganda: Mineralogical and chemical composition. *Chemical Journal* 35, 245–256.
[43]Pinheiro, P.G., Fabris, J.D., Mussel, W.N., Murad, E., Scorzelli, R.B., Garg, V.K., 2005, Benefeciation of a commercial kaolin from Mar Espanha, Minas Gervais, Brazil: chemistry and mineralogy. *Journal of South American Earth Sciences*, 20, 267-271.
[44]Pruett, R.J. and Murray, H.H., 1993, The mineralogical and geochemical controls that source rocks impose on sedimentary kaolin deposits. Pp. 149-170 in: *Kaolin Genesis and Utilization* (H.H. Murray, W. Bundy and C. Harvey, editors). Special Publication 1, The Clay Mineral Society, Indiana, USA.
[45]Pruett, R.J. and Pickering, Jr., S.M., 2006, Kaolin.Pp. 390-427 in: *Industrial Minerals and Rocks* (J.E. Kogel, N.C. Trivedi, J.M. Barker, and S.T. Krukowski, editors). Society for Mining, Metallurgy, and Exploration, Inc., Littleton, Colorado, USA.
[46]Rajala, H., 2012, The effect of size and structure of filler particles on paper properties. *International Pulp and Paper Technology*, *Tampere University*, 6 pp.
[47]Ramadan, T.M., Ibrahim, T.M., Said, A.D. and Baiumi, M., 2013, Application of remote sensing in exploration for uranium mineralization in Gabal El Sela area, South Eastern Desert, Egypt. *The Egyptian Journal of Remote Sensing and Space Sciences*, 16, 199-210.
[48]Rashed, M.A. and Amer, A.M., 1994, Geological and mineralogical studies on some West-Central Sinai kaolin deposits and their industrial applications. *Proc. 1st. Inter. Symp. on Industrial Applications of Clays, Cairo*, pp. 306-314.
[49]Refaie, F.A.Z., Abbas, R. and Fouad, H.F., 2020, Sustainable construction system with Egyptian metakaolin based geopolymer concrete sandwich panels. *Case Studies in Construction Materials*, 13, e00436.
[50]Rudnick, R.L. and Gao, S., 2004, Composition of the Continental Crust. In: Treatise on Geochemistry. Holland, H.D. and Turekian, K.K. (Editors), Elsevier, Amsterdam. 3: 1-64.
[51]Samidurai, R., Palaniandi, S., Thiagarajan, T., Kalyanasundara, N., Yossi, A., 2002, Foliar nutrition of peak on rice. *17th WCSS*, 1pp.
[52]Siddiqui, M.A., Ahmed, Z., Saleemi, A.A., 2005, Evaluation of Swat kaolin deposits of Pakistan for industrial uses. *Applied Clay Science* 29, 57–72.
[53]Spinaola, D.C.S., De Miranda, A., Macedo, D.A, Paskocimas, C.A. and Nascimento, R.M., 2019, Preparation of glass-ceramic materials using kaolin and oil well drilling wastes. *Journal of Materials Research and Technology*, 8(4), 3459-3465.
[54]Tassongwa, B.C. Nkoumbou, D. Njoya, A. Njoya, J.L. Tchop, J. Yvon and D. Njopwouo, 2014, Geochemical and mineralogical characteristics of the Mayouom kaolin deposit, West Cameroon. Earth Science Research; Vol. 3, No. 1;2014. 98-105 pp.
[55]Valaskova, M., Mikeska, M., Studentova, S. and Martynkova, G.S., 2018, Cordierite/Steatite ceramics sintered from talc, kaolin and vermiculites: comparison of natural and organovermiculites effect. *Materials Today: Proceedings*, 5, 88-95.
[56]Wallace W.E., Headley L.C., & Weber K.C., 1975, Dipalmitoyl lecithin surfactant adsorption by kaolin dust in vitro. J *Colloid Interface Science*, 51: 535–537.
[57]Wanas, H.A., 2011, The Lower Paleozoic rock units in Egypt: An overview, *Geoscience Frontiers*, 2(4), 491-507.
[58]Welton, J.E., 1984, SEM Petrology Atlas. AAPG Methods in Exploration Series, 4, 237 pp,
Tulsa.
[59]Weyer, S., Münker, C., Rehkämper, M. and Mezger, K., 2002, Determination of ultra-low Nb, Ta, Zr and Hf concentrations and the chondritic Zr/Hf and Nb/Ta ratios by isotope dilution analyses with multiple collector ICP-MS. Chem. Geol. 187, 295–313.
[60]Wilson, I.R., 2003, Kaolin Mining Annual Review 2002. The Mining Journal Ltd. Wouatong, G.A., 1997. Mineralogical study of weathering on the Bana Complex, West part of Cameroon. *Journal of Science, Hiroshima University series II*, 1–43pp.
[61]Yanni, N.N., 1988, Characteristics of some Carboniferous kaolin deposits, West Central Sinai. *Proc. Egypt. Acad.Sci*., v. 38:141-150.
[62]Zegeye, A., Yahaya, S., Fialips, C.I., White, M.L., Gray, N.D. and Manning, D.A.C., 2013, Refinement of industrial kaolin by microbial removal of iron-bearing impurities. *Applied Clay Science*, 86, 47-53.